# A MATHEMATICAL ANALYSIS OF THE INITIAL STABILITY OF A SHORT FEMORAL PROSTHESIS

*4th Semester Master Thesis*

By: Sandi Hupfeld

01-06-2016

AALBORG UNIVERSITET

AALBORG UNIVERSITY
MASTER THESIS

SCHOOL OF MEDICINE AND HEALTH

# A mathematical analysis of the initial stability of a short femoral prosthesis

$4^{th}$ SEMESTER MASTER THESIS

BIOMEDICAL ENGINEERING AND INFORMATICS

GROUP 16GR10402


***Supervisors:***
Carsten Dahl Mørch
Karl Brian Nielsen

***Author:***
Sandi Hupfeld

***Clinical supervisor:***
Poul Torben Nielsen



**Pages**: 89
**Appendix**: 1
**Concluded**: June 1, 2016

# Abstract

**Purpose:**

Hip arthroplasty is a common surgical procedure to relieve pain caused by disease or hip fractions etc.. The durability of the procedure is finite, which makes treatment of younger patients challenging. Based on this, research with short femoral stems in order to preserve bone for multiple revisions have been made. One of these is the newly developed Primoris stem. This is fixated by bone compaction, which in theory provides a good initial stability. But the preconditions of the host bone are crucial for obtaining a successful result, however no studies have been made in order to investigate this.
The aim of this thesis was to analyse the initial stability of Primoris, based on the compressive behaviour of bone tissue and thereby create representative mathematical models to analyse the effect of different preconditions of the host bone.

**Methods:**

As the mechanical behaviour of bone tissue depends on the relative density $\rho_r$ and additionally changes during compaction, a mathematical expression was derived for $\rho_r$= 0.2 to $\rho_r$ = 0.6, in order to obtain results which rely on the true behaviour of the bone tissue. For analysing the stability by estimating the pull-out force, a Finite Element (FE) model was developed using LS-DYNA. This method allows a simulation of the insertion process in 3D of where the impact of different preconditions of the host bone can be estimated. But as the reliability of the results from the FE model is difficult to determine, a simplified analytical model was created to provide a basic understanding of the process and thereby be able to develop the FE model.

**Results:**

The initial process of developing a mathematical expression in order to describe the compressive behaviour of the bone tissue, followed the trend found in the literature and provided the basis for the two models. The analytical model showed that the lowest contact pressure obtained was at $\rho_r$ = 0.2, where only 7 % compaction was obtained compared with 94.7 % at $\rho_r$ = 0.6. It was also found that the friction between the bone and stem had a major impact on the pull-out force. Both the analytical model and the FE model showed that various $\rho_r$ are of great importance for succes, as an increase in $\rho_r$ contributes with a higher pull-out force. They also showed higher pull-out force when changing the conical angle from $\theta$=3.5°to $\theta$=3.5°.

**Conclusion:**

There were a significant similarity between the results obtained from the models when changing the preconditions, of which it can be concluded that the FE model demonstrated the ability of analysing different preconditions and thereby estimating the initial stability. This can be useful for a qualitative prediction of the surgical procedure. The parameter effecting the stability the most was $\rho_r$, as a lower $\rho_r$ resulted in lower pull-out force, and thereby an inferior stability. But it was also seen that the geometry of the stem had an impact of the result.

# Preface

This master thesis is made by Sandi Hupfeld during the $4^{th}$ semester Master in Biomedical Engineering and Informatics at Aalborg University, during the period from February 2016 to June 2016.

The topic of this project was proposed by chief surgeon in orthopaedics, Poul Torben Nielsen Cand. Med. PhD, from Aalborg Universitetshospital (AUH). It emerged from a current problem in relation to the insertion of a new femoral prosthesis, where the fixation method is bone compaction in order to obtain a good initial stability. The objective with this thesis was to analyse the mechanical behaviour of bone during compression and thereby construct a mathematical model in order to estimate the initial stability. Though the area of mechanics was far from biomedical engineering, it has been an exciting and educational process to combine these fields of study, and to obtain an understanding of how the two fields of research are interrelated.

References appears according to the Harvard method [Last name, year], and are gathered in a bibliography found in the end of the thesis. If several authors, only the first author is listed followed by et al.. Reference prior the period refers to the sentence and references after the period refers to the whole section. Figures, equations and tables are numbered according to the chapter. Figures without references are created by the author.

Gratitude goes towards project supervisor Karl Brian Nielsen for his help with providing the essential mechanical understanding for carrying out this thesis and guidance during the mathematical modelling. Gratitude is also given to Poul Torben Nielsen for providing clinical informations and materials.

Sandi Hupfeld

# Contents

**Chapter 1 Introduction** 1
1.1 Initiating problem . . . 2

**I Problem analysis** 3

**Chapter 2 The composition and structures of the hip** 5
2.1 Anatomy of the hip . . . 5
2.1.1 Pelvis . . . 6
2.1.2 Femur . . . 6
2.2 Bone composition . . . 8
2.2.1 Bone cells . . . 9
2.3 Structure of compact- and trabecular bone . . . 10

**Chapter 3 Hip arthroplasty** 13
3.1 Predisposing factors . . . 14
3.1.1 Hip arthrosis . . . 14
3.1.2 Hip fractions . . . 14
3.1.3 Avascular necrosis and rheumatoid arthritis . . . 14
3.2 Femoral prosthesis . . . 15
3.2.1 Fixation methods . . . 16
3.3 Primoris stem . . . 17
3.3.1 Geometric foundation of the stem . . . 17
3.3.2 Templating . . . 18

**Chapter 4 Summary** 21
4.1 Problem statement: . . . 21

**II Problem solution** 23

**Chapter 5 Modelling methods** 25
5.1 Mechanical behaviour of trabecular bone . . . 26
5.1.1 Mechanical assumptions . . . 29
5.2 Compressive behaviour of bone tissue . . . 29

5.2.1 Derivation of an expression for the compressive behaviour . . . . . . . . 29

**Chapter 6 Analytical model** **33**
6.1 Geometric interpretations . . . . . . . . . . . . . . . . . . . . . . . . . . . . . . . . . 33
6.1.1 Contact pressure between stem and bone . . . . . . . . . . . . . . . . . . 34
6.2 Process of bone compaction . . . . . . . . . . . . . . . . . . . . . . . . . . . . . . . 35
6.2.1 Pull-out force . . . . . . . . . . . . . . . . . . . . . . . . . . . . . . . . . . . . . . 36

**Chapter 7 Analytic parameter study of preconditions** **39**
7.1 Contact pressure and maximum bone compaction . . . . . . . . . . . . . . . . . . 40
7.2 Effect of varying friction and angle of the stem . . . . . . . . . . . . . . . . . . . . 43
7.2.1 Critical angle of the stem . . . . . . . . . . . . . . . . . . . . . . . . . . . . . 45
7.3 Effect of varying radius of the trabecular bone . . . . . . . . . . . . . . . . . . . . 45

**Chapter 8 Finite Element modelling** **47**
8.1 FE theory . . . . . . . . . . . . . . . . . . . . . . . . . . . . . . . . . . . . . . . . . . 47
8.1.1 Dynamic equilibrium in FE domain . . . . . . . . . . . . . . . . . . . . . . . 48
8.1.2 Potential energy in the model . . . . . . . . . . . . . . . . . . . . . . . . . . 49
8.1.3 Geometry update through FE loop . . . . . . . . . . . . . . . . . . . . . . . 50
8.2 Creating the model in LS-DYNA . . . . . . . . . . . . . . . . . . . . . . . . . . . . . 51
8.3 Preliminary FE model . . . . . . . . . . . . . . . . . . . . . . . . . . . . . . . . . . . 54
8.4 Simulating different densities . . . . . . . . . . . . . . . . . . . . . . . . . . . . . . 56
8.5 Simulating geometric changes . . . . . . . . . . . . . . . . . . . . . . . . . . . . . . 58
8.5.1 Simulating different yield strength . . . . . . . . . . . . . . . . . . . . . . . . 58

**Chapter 9 Results** **61**

**III Synthesis** **65**

**Chapter 10 Discussion** **67**
10.1 Methods . . . . . . . . . . . . . . . . . . . . . . . . . . . . . . . . . . . . . . . . . . 67
10.2 Results . . . . . . . . . . . . . . . . . . . . . . . . . . . . . . . . . . . . . . . . . . . 68
10.3 Future perspective . . . . . . . . . . . . . . . . . . . . . . . . . . . . . . . . . . . . 69

**Chapter 11 Conclusion** **71**

**Bibliography** **73**

**IV Appendix** **77**

**Appendix A X-ray for geometric determinations** **79**

CHAPTER

# 1 Introduction

In Denmark the procedure of hip arthroplasty has been performed commonly at the majority of the Orthopaedic Surgery departments since 1970.[Per Kjærsgaard-Andersen and Søballe, 2006] The procedure is offered to patients with hip pain, of which medical treatment no longer provides a proper relief. These patients often suffers from hip arthrosis or have been exposed to fractions in the hip. The medical term for the hip is the acetabulofemoral joint which consists of the thigh bone (femur), and the hip bone (pelvis). Pelvis and the femoral head are attached in the socket (acetabulum).[Frederic Martini and Bartholomew, 2012][Dieppe and Lohmander, 2005]

During the surgical procedure of hip arthroplasty most of the proximal part of femur, and the outer layer of acetabulum are removed and replaced with an artificial ball and socket. The ball is attached to a stem which is inserted inside the shaft (diaphysis) of femur. In order to fixate the stem there exist two methods of which the most common is by the usage of bone cement. This involves removal of the spongy bone (trabecular bone) by drilling a hole in femur at the size of the stem and filling it with bone cement to retain the stem. The other fixation method is based on biological fixation of where knowledge about the composition of the bone tissue is utilized. Bone is composed by different types of cells which both degrades and rebuilds the tissue when damaged. Instead of removing the trabecular bone it is compacted with conical stems of increasing sizes. This induces that new bone will grow around and into the surface of the stem and thereby support it, which leads to a good initial stability of the prosthesis.[Ashby and Gibson, 1999] [Søren Kold and Søballe, 2003] The applied method and choice of femoral stem are depending on the individual patient since factors as age, sex and bone quality are of influence.[John R. Green and Balas, 1997]

Earlier the surgery of hip arthroplasty was only offered to patients above 60, since the lifespan of the prosthesis is finite and a revision is required after approximately 15 years. As a consequence of removing most of the proximal part of femur, the amount of bone for a revision after the surgery is limited, which is why only one revision is possible. This is found to be very critical when operating younger patients.[Boris Zelle and Krettek, 2004] In order to avoid these problems, studies with short femoral stems have been made. This type of stem is inserted with removal of a smaller amount of bone, which provides the possibility to preserve bone for multiple revisions, and thereby perform the procedure on younger patients. [Søren Kold and Søballe, 2004][Søren Kold and Søballe, 2003]

One of the short femoral stems is the newly developed Primoris Stem, of which the geometry is based on morphological analysis of several radiographic of femur, in order to obtain the best fit.[Peter Walker and Casas, 2005] The fixation of Primoris is based on bone compaction, which in theory provides a good initial stability. But the conditions of the host bone is essential for the bone compaction to provide a successful result. Since Primoris is a new clinical approach, the influence of different precondition of the host bone has not been investigated, therefore no indications of which anatomical and mechanical preconditions that are crucial for obtaining the best initial stability exist. [Søren Kold and Søballe, 2004][Søren Kold and Søballe, 2003]

Assuming that the initial stability can be described as the pull-out force of the stem from the bone, this thesis proposes a mathematical approach for investigating the initial stability under various preconditions. This method allows an estimation of the pull-out force when changing essential parameters, and it provides an insight of which preconditions that leads to the best initial stability.

An understanding of the compressive behaviour of bone tissue and the physical effect of the problem can be obtained by creating an analytical model, which is a simplified model resulting in a closed-form solution. The analytical model can be used as a basis for creating a numerical model which allows more complex and time-dependent examinations. A numerical method to analyse this is the Finite Element method, which is often used for evaluating biomechanical problems.

To construct the mathematical models for analysing the initial stability, knowledge about the hip, the bone composition and the surgical procedure is needed.

This leads to the following initiating problem:

## 1.1 Initiating problem

*How is the hip and bone tissue constructed and what are the basic principles behind hip arthroplasty?*

# Part I

# Problem analysis

CHAPTER

# 2 The composition and structures of the hip

In order to create a mathematical model to simulate the compressive behaviour of bone tissue when inserting the femoral stem, it is necessary to have an understanding of the anatomy and physiology of the human hip. Knowledge about the composition of the bone and the mechanical behaviour is also important in order to calculate the compaction process, which is why the basic principles is described in the following chapter.

## 2.1 Anatomy of the hip

The human hip is a ball-and-socket joint which supports the weight of the body and forms the transition from the torso to the lower limbs. The hip consists of pelvis and the femoral head, of where the femoral head articulates with acetabulum pelvis creating the hip joint also referred to as the acetabulofemoral joint as illustrated in figure 2.1.[Frederic Martini and Bartholomew, 2012]Per Kjærsgaard-Andersen and Søballe [2006]

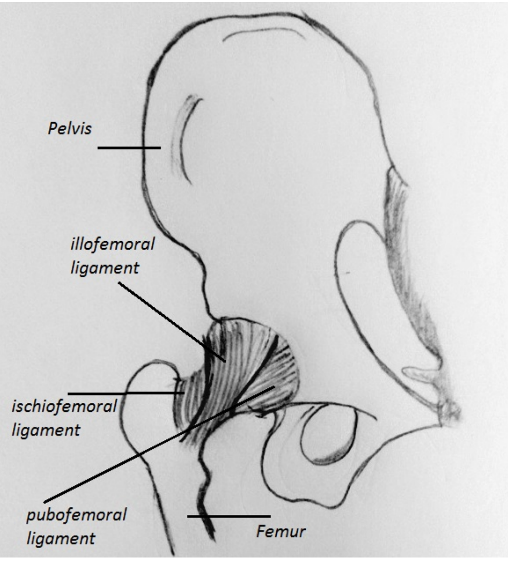


***Figure 2.1.*** Illustration of the acetabulofemoral joint composed by pelvis and femur and stabilised by ligaments.

Fibrocartilage is located inside acetabulum which protects the bones and ensures a friction-free movement. The joint is stabilised by the illofemoral ligament, ischiofemoral ligament, pubofemoral ligament and iliofemoral ligament.[Frederic Martini and Bartholomew, 2012]

### 2.1.1 Pelvis

Pelvis is posterior formed by sacrum which is connected to the lumbar vertebrae L5 and coccyx, as illustrated in figure 2.2. Anterior pelvis consists of the pelvic bones which are divided into the three bones ilium, ischium and pubis. These are separate bones until puberty. The pelvic bones are referred to as the pelvic girdle. Lateral is the acetabulum, which is connected to the femoral head. The surface of acetabulum is called the lunate surface because of the moon shaped form.[Frederic Martini and Bartholomew, 2012]

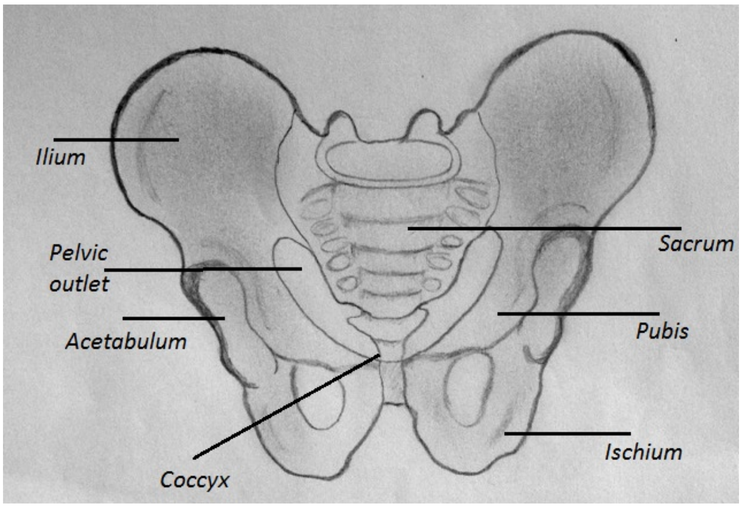


***Figure 2.2.*** Illustration of the pelvic girdle composed by different bones and acetabulum witch is a part of the acetabulofemoral joint.

The shape and size of pelvis differs from male to female because of the ability to deliver birth. The female pelvic is lower, the outlet is wider and more circular and the angle between the pubic bones are broader.[Frederic Martini and Bartholomew, 2012]

### 2.1.2 Femur

Femur is the largest and heaviest bone in the human body and located in the thigh. The size and general appearance variates for each individual and are dependent on e.g. gender, weight, age etc..[Frederic Martini and Bartholomew, 2012]Per Kjærsgaard-Andersen and Søballe [2006]

Femur consists of the epiphysis, which is located at each end of the diaphysis, the shaft of femur. The anatomically structures of the right femur shown anterior is seen in figure 2.3.[Frederic Martini and Bartholomew, 2012]Per Kjærsgaard-Andersen and Søballe [2006]

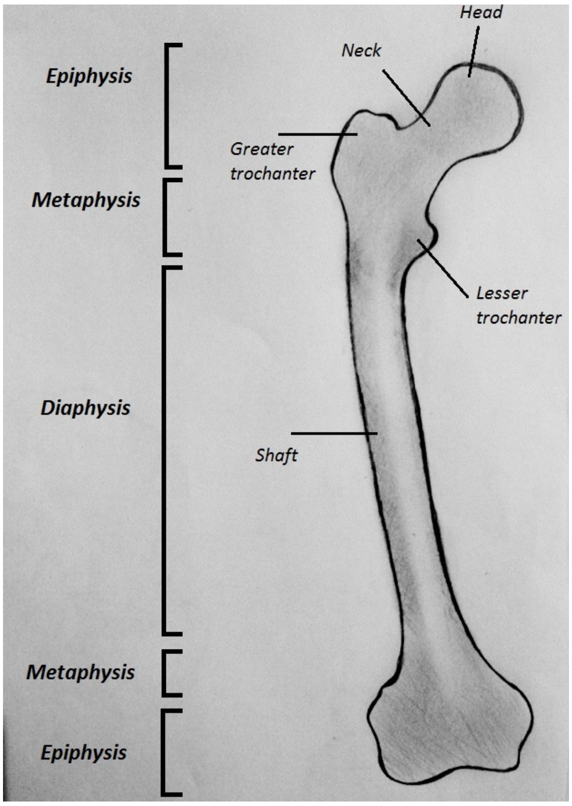


***Figure 2.3.*** Illustration of the right femur showing the different anatomically parts anterior.

The femoral neck is attached to the diaphysis with an angle at approximate 125°, separated by the metaphysis. At the proximal epiphysis is the femoral head, the neck, and the greather and lesser trochanter of which large tendons are attached to. The distal part of femur articulates with tibia creating the knee joint.[Frederic Martini and Bartholomew, 2012]Per Kjærsgaard-Andersen and Søballe [2006]

## 2.2 Bone composition

Focus of this section is the bone structures and composition of femur, since these are essential for creating the mathematical models and thereby provide an understanding of the compaction process. As seen in figure 2.4 femur consists of different types of bone tissue which contains different types of bone cells. The surface is covered by periosteum, a membrane that covers the entire bone except at the joint cavity, with the purpose of isolating and hosting bone cells. The epiphysis is composed by trabecular bone and the diaphysis by compact bone and the madullary cavity which contains bone marrow.[Gibson, 1985][Frederic Martini and Bartholomew, 2012][M. Doblare and Gomez, 2003]

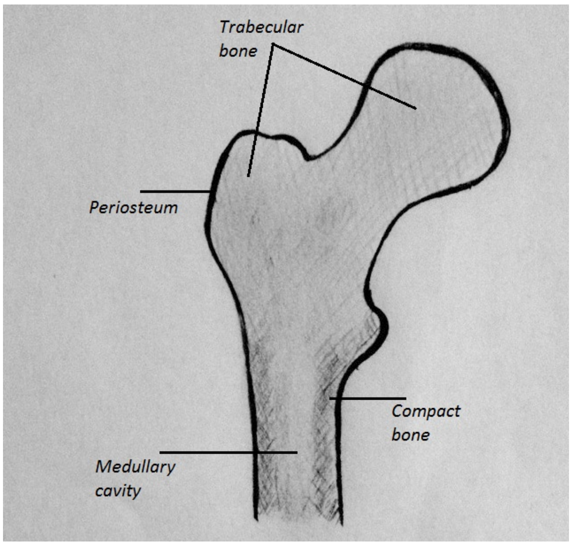


***Figure 2.4.*** The images shows the composition of femur and the location of the different types of bone.

The bone tissue is composed by a matrix consisting of approximately 35 % organic material, 45 % inorganic material, and 20 % water. The matrix is similar in compact and trabecular bone, but with a different volume fraction.

The organic matrix is constructed by proteins i.e. collagen and forms the fundamental matrix of which the inorganic materials are applied, resulting in a combined matrix with the characteristics of both strength and flexibility. The inorganic matrix is composed by calcium salts i.e. crystaline hydroxyapatite ($Ca_{10}(PO_4)_6OH_2$) with a size of 5540 nm and amorphous phosphate which contributes with the stiffness of the final matrix. The space between the bone matrix is filled with bone marrow. The volume of bone can be calculated according to equation (2.1), as the total volume minus the volume of the cavities.[Gibson, 1985][Frederic Martini and Bartholomew, 2012][M. Doblare and Gomez, 2003]

$$V_{bone} = V_{tot} - V_{cav} \tag{2.1}$$

The porosity [p] of the bone can then be determined by equation (2.2).

$$p = 1 - V_{bone}/V_{tot} \tag{2.2}$$

of which the $V_{bone}/V_{tot}$ is defined as the bone volume fraction. This gives that the bone is more porous with lower volume fraction. [Gibson, 1985]

In this case the marrow will not be taken into consideration, because it does not have an influence on the mechanical behaviour of the bone tissue in the hip. The $V_{bone}$ will then be calculated as the organic materials + inorganic materials.[Gibson, 1985][Frederic Martini and Bartholomew, 2012][M. Doblare and Gomez, 2003]

### 2.2.1 Bone cells

The bone matrix is constructed, maintained and decomposed by different type of bone cells: Osteoblasts, osteocytes, osteoprogenitor, and osteoclasts. These does not affect the mechanical behaviour of the tissue, but are very important in order to understand the ongoing processes inside the bone tissue, and how it is rebuild after the compaction.

Osteoblasts are located at the periosteum in the marrow and are responsible of ossification which is the process of creating new bone matrix. The osteoblasts produces the organic compounds of the matrix and catalyses the addition of calcium creating the final bone matrix. [Alexandre Terrier, 2005] [Frederic Martini and Bartholomew, 2012]

When the osteoblasts are fully surrounded by completed bone matrix they are called osteocytes, which are the most frequent type of bone cells located in the small cavities, lacunae. They dynamically maintains the components of the matrix and if the matrix is damaged they may participate in bone remodelling caused by disruptions of their attachments and thereby released from the lacunae.[Alexandre Terrier, 2005] [Frederic Martini and Bartholomew, 2012]

Osteoprogenitor cells are stem cells found i.a. in periosteum and bone marrow and when exposed to a certain biological signal they are able to differentiate into osteoblasts. This process establish the quantity of osteoblasts and is of great importance in the case of bone fractions.[Alexandre Terrier, 2005] [Frederic Martini and Bartholomew, 2012]

The last type of bone cells are the osteoclasts which are the cells that demineralises and removes bone matrix by releasing acids and proteolytic enzymes. They originates from the bone marrow and are affected by hormones which indicates the location and amount of bone tissue to be removed. This process is essential for maintaining the right concentration of calcium and phosphate and the amount of bone matrix. If the relation between the osteoclasts and osteoblasts is damaged, it would result in either a more massive bone or a weaker bone. [Alexandre Terrier, 2005] [Frederic Martini and Bartholomew, 2012]

The focus of this thesis is as mentioned the diaphysis of femur which as described in section 2.2 primary consists of trabecular bone and compact bone. The periosteum and marrow are not taken into account in the following descriptions and calculations since it does not have a significant impact on the results.

## 2.3 Structure of compact- and trabecular bone

The outer layer of femur consists of compact bone, which is composed by the same matrix as trabecular bone but with a higher density, and osteon as the functional unit. The osteon consists of central canals (osteonic) with a size of 50 $\mu$m containing blood vessels, and are enclosed by concentric rings of bone matrix. The space between these rings is the lacunae where the osteocytes are located. The volume fraction of compact bone is higher than of trabecular bone, and is classified if above 70 %.[Gibson, 1985][Ashby and Gibson, 1999][Alexandre Terrier, 2005]

When the volume fraction of the bone tissue becomes less than 70 % it is classified as trabecular bone. This means that the bone tissue is weaker and more flexible than of compact bone but suitable for the execution of biological processes. It is localized in the areas of the bone which is not exposed to high mechanical stresses, as in the diaphysis of femur. The relative density $^{\rho}/_{\rho^*}$ ($\rho_r$) lies between 0.05 - 0.7, of which the visual appearance of the matrix is spongy and consists of open cells, which differs depending on the relative density. At the lowest relative density the cells are open and reminds of rods, but when the relative density increases the cells becomes almost closed and reminds of plates. [Ashby and Gibson, 1999][Gibson, 1985][Alexandre Terrier, 2005]

The trabecular bone is composed by trabeculae as the functional unit which have a size of 50 $\mu$m. These are orientated along the stress direction and grows in response to the stress because of the piezoelectric property, which means that areas exposed to high stress have a higher density than areas exposed to low stress. [Gibson, 1985][Ashby and Gibson, 1999][Alexandre Terrier, 2005]

Both kind of tissue are considered to have a viscoelastic behaviour which means that the behaviour of the materials are both viscous which changes shape depending on the container and elastic. The elasticity can be described by finding the elastic modulus also called Young's modulus [E] using equation (2.3), which is the relation between the stress $\sigma$ and strain $\varepsilon$:[Ashby and Gibson, 1999][Gibson, 1985][Alexandre Terrier, 2005]

$$E = \sigma / \varepsilon \tag{2.3}$$

E is an expression for the stiffness of the material and how well it is able to resist deformation. The behaviour of the trabecular bone is not linear-elastic which is a result of the walls of the cells is bended. When the walls is compressed and it collapses the behaviour becomes plastic. The collapse can occur either by elastic buckling which is the primary behaviour if the $\rho_r$ is low or plastic yielding.[Søren Kold and Søballe, 2003][Ashby and Gibson, 1999][Gibson, 1985][Alexandre Terrier, 2005]

The mechanical behaviour of trabecular bone is depending on $\rho_r$. As the bone is anisotropic, the behaviour is different in the radial direction than of the axial direction. Since this thesis only analyses the behaviour of the bone when it is compacted, it is only the behaviour in the radial direction that is of interest. [Søren Kold and Søballe, 2003][Ashby and Gibson, 1999][Gibson, 1985][Alexandre Terrier, 2005]

As fractures and diseases frequently occurs in the hip, a hip prosthesis is a well used method for reducing the pain, which is why several prosthesis and insertions methods exist. As bone tissue possesses the ability to adapt when changing the environment or applying a different mechanical load, research have been made with biological fixation of the prosthesis. This method requires knowledge about the composition of the bone tissue in the hip and the corresponding mechanical behaviour.

CHAPTER

# 3 Hip arthroplasty

Total hip arthroplasty is the definition of the procedure when diseased cartilage of the acetabulum is rasped of and replaced with a socket inside acetabulum and attached to pelvis, which fit the femoral head. The top of femur is cut of and replaced by a stem inserted into the trabecular bone, and a metal ball joint as the femoral head. The surgical procedure of hip arthroplasty is shown in figure 3.1.[Per Kjærsgaard-Andersen and Søballe, 2006]

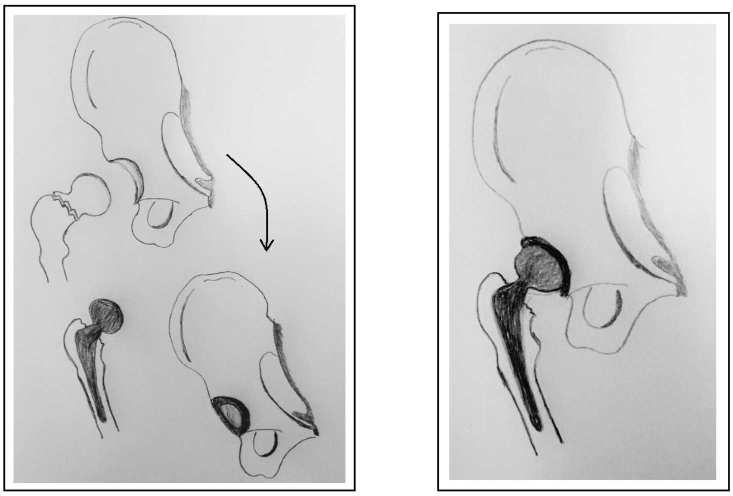

***Figure 3.1.*** The procedure of a total hip arthroplasty where the femoral head, neck and acetabulum are replaced by a prosthesis.

At first the femoral head is dislocated from acetabulum and then sawed off. The surface of the acetabulum will be abraded and a artificial acetabular cup is inserted. Then a hole is made inside femur down through the diaphysis and the femoral stem is inserted by either compaction or cement and the joint is put back into the right position. If only the femoral head and neck are replaced by a prosthesis it is called a hemiarthroplasty.[Per Kjærsgaard-Andersen and Søballe, 2006]

## 3.1 Predisposing factors

There are several conditions that may results in hip arthroplasty as the best solution, in order to achieve pain relief and restoration of mobility for the patients. The most common conditions are hip arthrosis, femoral fractures, avascular necrosis and rheumatoid arthritis which are described in the sections below.

### 3.1.1 Hip arthrosis

The most common reason for hip arthroplasty is hip arthrosis which constitutes approximately 80 % of all cases in Denmark.[Per Kjærsgaard-Andersen and Søballe, 2006] It is a chronic disorder where the joint cartilage is degraded which causes pain when using the hip. Normally the cartilage cells is constructed by a matrix of collagen and proteoglycans which decreases friction in the joint, but the arthrosis degrades the matrix resulting in morphological changes and a loss of the volume of the cartilage. The joint will eventually become deform where the femoral head is unable to move freely and thereby stiffen increasingly. Eventually the pain will progressively occur even when the patient is at rest, joint movement will be difficult, and due to the decreasing cartilage layer, the leg will be shortened. The arthrosis is divided into primary and secondary, of which the cause is unknown for the primary arthrosis but the risk increases with age and excessive weigh. The secondary arthrosis is caused by another disorder such as congenital malformations, inflammation in the joint, earlier fractions etc..[Dieppe and Lohmander, 2005]

### 3.1.2 Hip fractions

Hip fractions are the second most frequent cause for hip arthroplasty in Denmark and constitutes approximately 11 % of all cases. The fractions are located at the proximal part of femur and can be divided into three general categories.[Per Kjærsgaard-Andersen and Søballe, 2006]

The most common is femoral neck fractures, which is intracapsular and located between the femoral head and the intertrochanteric region. According to the *Garden classification system*, these can be subdivided into incomplete fractions, complete and nondisplaced, complete and partially displaced and completely displaced. Intertrochanteric fractures and subtrochanteric fractures are both extracapsular fractures of which subtrochanteric are located at the methaphysis and the top of the diaphysis. This type can be divided into stable trochanter, unstable trochanter and transtrochanteric, according to the risk of fracture displacement and location.[Claus Munk Jensen and Villadsen, 2008]

### 3.1.3 Avascular necrosis and rheumatoid arthritis

Avascular necrosis and rheumatoid arthritis are less common diseases which may result in hip arthroplasty. Avascular necrosis primary affects the epiphysis of long bones which in this case is the femoral head. It constitutes approximately 2.6 % of all cases and reduces the blood supply which leads to degraded trabecular bone and bone marrow.

The process happens very fast and within 24 hours, the osteocytes, osteoclasts, and osteoblasts starts to decompose. At the early stages I and II, symptoms may not be present and the treatment will at first be joint preservation surgery. But when it becomes more progressive and painful at stage III and IV the acetabulofemoral joint will be deform and eventually collapse, which will result in hip arthroplasty as the only treatment.[Mont and Hungerford, 1995] [Claus Munk Jensen and Villadsen, 2008]

Rheumatoid arthritis constitutes approximately 1.5 % of all hip cases and most frequently affects women. It is a autoimmune chronic inflammatory joint disease effecting the synovial and cartilage cells in the joint, resulting in deformation of the joint and an erosion of the femoral head. The symptoms is constant pain, fatigue, swelling and limitation of motion.[Scott and Wolfe, 2010] [Claus Munk Jensen and Villadsen, 2008]

## 3.2 Femoral prosthesis

In Denmark the procedure of hip arthroplasty has been performed commonly at the majority of the Orthopaedic Surgery departments since 1970 where the cemented fixation was the only method.[Per Kjærsgaard-Andersen and Søballe, 2006] Today, more than 100 different femoral prosthesis exists, of which the biggest difference is the length and shape of the stem and consequently how much of femur that has to be removed. Some of the different lengths are shown in figure 3.2, where the line indicates how much of femur that is removed.[Per Kjærsgaard-Andersen and Søballe, 2006][Den Ortopædiske Fællesdatabase, 2013]

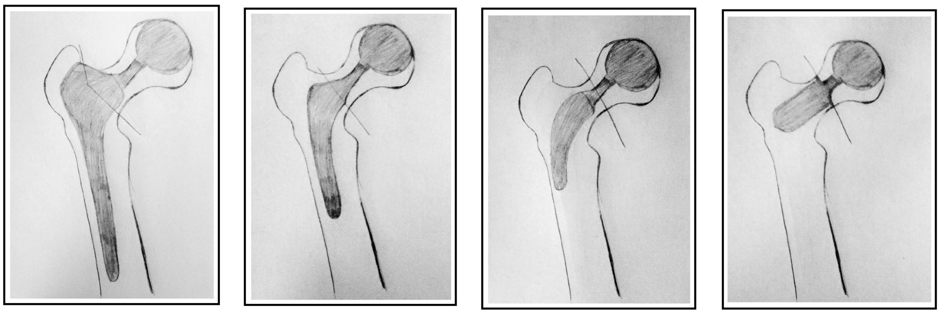

***Figure 3.2.*** The figure shows four different types of femoral stems with different length. The line indicates where femur is sawn off.

The stems exist with different coating and are either categorised as cemented hip arthroplasty, uncemented hip arthroplasty or hybrid hip arthroplasty.[Den Ortopædiske Fællesdatabase, 2013] The applied method and choice of prosthesis are dependent on the individual patient since factors as age, sex and bone quality are of influence.[Per Kjærsgaard-Andersen and Søballe, 2006]

### 3.2.1 Fixation methods

The fixation of the prosthesis when inserted into femur is depending on the design of the prosthesis, the placement inside femur, loading from the weight of the patient and most important the quality and quantity of bone tissue. All these factors influence the result of the stability and durability of the prosthesis when the patient starts using the hip, and the prosthesis and host bone is exposed to stress and strain. The existing fixation techniques are either with the usage of bone cement or biologic which is either by bone compaction or press fit.[John R. Green and Balas, 1997] [Per Kjærsgaard-Andersen and Søballe, 2006]

If the prosthesis is fixated with bone cement, all the trabecular bone from the medulla cavity and the walls of the diaphysis is removed with a drill bit in the size of the prosthesis. The residues of the trabecular bone that has been loosened when drilling are removed and the hole is filled with bone cement. A stem is placed in the middle of the cement and hammered into place to ensure that the stem is placed properly. [John R. Green and Balas, 1997]

The technique behind compaction and press fit is a bit different than when using bone cement. The intention with these methods is to achieve a biological fixation of the stem. When the trabecular bone is damaged, it is decomposed by osteoclasts and rebuild by osteoblasts. As described in section 2.2 the osteoblasts creates bone matrix in response to stress, which will appear when the prosthesis is inserted and the patient starts using the joint and the prosthesis is exposed to load. The new bone matrix will then grow around the prosthesis which will support it. If the prosthesis is inserted by press-fit, a pre-operatively cavity 1 mm smaller than the size of the prosthesis is drilled, and the prosthesis is pressed into this cavity.[Per Kjærsgaard-Andersen and Søballe, 2006]

The surgical procedure of bone compaction starts with drilling a small pilot hole in the middle of femur. Then the trabecular bone is sequentially removed and dilated with smooth conical stems in increasing sizes. The first stem are with barbs, which compacts and pushes a small amount of the trabecular bone down in the cavity simultaneously. The next sizes of the stems are smooth in order to compact the remaining trabecular bone as much as possible without damaging the compact bone, and the stem is inserted into the cavity.Søren Kold and Søballe [2004]

## 3.3 Primoris stem

As described previously the epiphysis and methaphysis of femur are removed during the insertion of the femoral prosthesis. This is found to be very critical if a revision is needed, because of the lack of methaphysial bone for a revision. It is especially critical when the procedure is necessary for younger patients, as the prosthesis have a certain life span which is why a prosthesis previously was not an option. As a solution to this problem, the Primoris stem has been developed. This method allows the ability to preserve metaphysial bone in order to increase the possibility of multiple revisions, and therefore the ability to operate younger patients.Søren Kold and Søballe [2004]

### 3.3.1 Geometric foundation of the stem

As described in section 3.3, Primoris exist in different sizes. This study is based on the most frequently used, which is the 24 mm. The geometry of the 24 mm is illustrates in figure 3.3 frontal and median, indicated with 120 % scale.

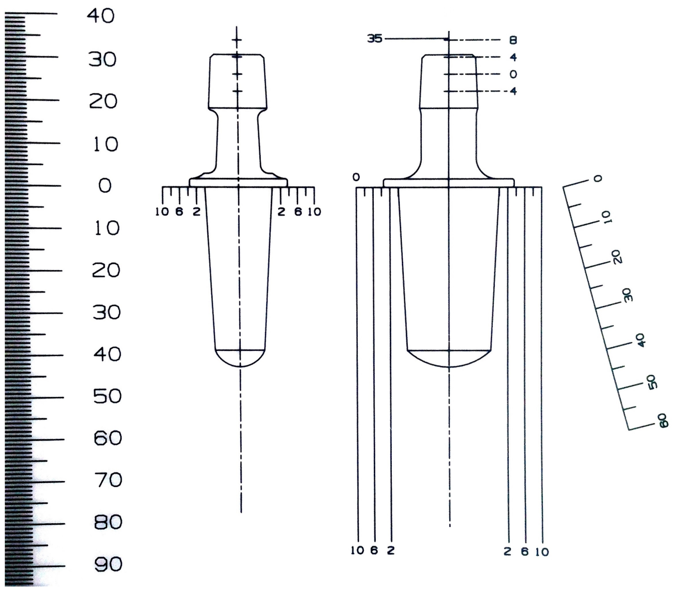


***Figure 3.3.*** The geometry of Primoris at the size 24 seen median (left) and frontal (right).

The top diameter frontal is 24 mm and the bottom is 19 mm. The length of the stem is 40 mm, which gives a conical angle at approximately $\theta = 3.5$ °.

A x-ray of the Primoris is shown in figure 3.4, which illustrates the placement and the geometry in relation to the bone.

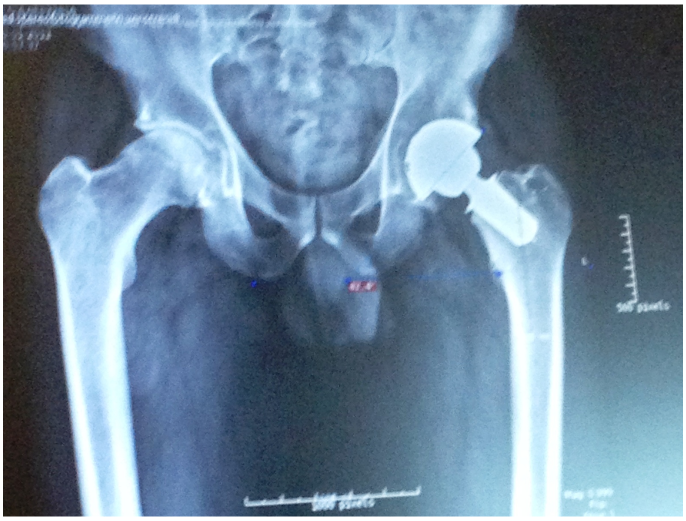

***Figure 3.4.*** X-ray of the hip where the Primoris stem is inserted in the left femur.

Compared to other short stems, the shape of Primoris is unique and designed from the geometry of the methaphysis, based on an average study made by [Peter Walker and Casas, 2005]. The study investigates the anatomical shape of radiographic of 100 proximal femur. Morphological analysis of the radiographic contributed to the shape and on the basis of a cluster analysis, 12 different average sizes of the methaphysis were defined. These results are applied on Primoris, which is designed in 5 different sizes with a diameter at 22 mm, 24 mm, 26 mm, 28 mm and 30 mm in order to achieve an accurate fit in the methaphysis depending on the patient. This specific shape provides a better fit and ensures immediately postoperative fixation. [Peter Walker and Casas, 2005] In order to secure a better bone ingrowth the surface of the prosthesis is beaded and covered by titanium and bonemaster.

### 3.3.2 Templating

The fixation of the stem and the primary stability are also dependent on the size of the stem and the conditions of the host bone, such as relative density and geometry. This is determined preoperative by templating based on an anteroposterior x-ray image of the hip, as seen in figure 3.5.[Larry W. Carter and Young, 1995][Per Kjærsgaard-Andersen and Søballe, 2006]

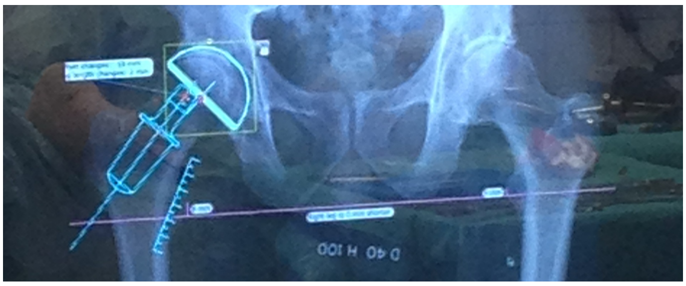

***Figure 3.5.*** Anteroposterior x-ray of the hip for templating the insertion of the hip prosthesis in the right hip.

This allows for a visual anticipation of the individual biomechanics in the hip such as center of rotation, which should provide an idea of the correct placement. The diameter of the metaphysis is used to determine the size of the stem and thus the fit of the stem. The sizing of the stem is very important, as an under dimensioned stem would result in poor initial fixation and conversely femoral fractures may occur. The placement and size is essential in order to achieve a stable prosthesis and avoid a mechanical loss of fixation over time.[Larry W. Carter and Young, 1995][Per Kjærsgaard-Andersen and Søballe, 2006]

The templating is performed on visual basis, and the result is consequently depending on experience and practice of the surgeon, since no precise procedure exist because of the major difference in each patient. [Larry W. Carter and Young, 1995] But as the biomechanics of the hip is depending on the mechanical behaviour of the bone, which again is depending on age, size, bone density etc. the result of the templating is only guiding, since the x-ray does not insinuate any mechanical behaviour when the stem is inserted. Studies regarding the accuracy of the size predicted preoperative during templating and the actual stem chosen during the surgery have been made for uncemented stems. These shows that the predicted size is inaccurate 50% of the times, which means that the final decision have to be made of the surgeon during the surgery.[Larry W. Carter and Young, 1995][Per Kjærsgaard-Andersen and Søballe, 2006]

As mentioned a wrong size may result in poor fixation, which is why it is very important that the size of the stem is proper for the individual patient.[Larry W. Carter and Young, 1995][Per Kjærsgaard-Andersen and Søballe, 2006] As the Primoris is a relative new initiative, the conditions for achieving the best postoperative stability and long term fixation have not been investigated.

CHAPTER

# 4 Summary

Several conditions can cause pain in the hip, of which hip arthrosis is the most common. When medical treatment no longer reduces the pain, a hip arthroplasty is offered to the patient. This procedure consists of an acetabular cup and a femoral prosthesis of where a stem is inserted into the trabecular bone of femur.

As the durability of the prosthesis is finite, which makes the treatment of younger patients difficult, research have been made with short femoral stems in order to preserve bone for multiple revisions. A newly developed short femoral stem is Primoris, which is fixated by bone compaction, using smooth conical stems of increasing sizes. This sequentially expands a region of the bone, equivalent to the femoral stem, resulting in a pressure on the stem which in theory should provide a good initial stability of the stem. The conditions of the host bone is crucial in order to achieve initial stability due to the amount of bone compaction and thereby obtaining a successful result. As the only existing method to determine the preconditions of the host bone is by templating, which provides a visual conception of the anatomical and mechanical conditions, it is difficult to determine if the host bone is acceptable, and which size of the prosthesis that provides the best result. Additionally, no studies have been made of which preconditions that are necessary for the procedure to be successful.

It is known that parameters as the relative density of the bone tissue, and the amount of bone compaction is of great importance for a successful procedure. Furthermore the geometric design of the prosthesis due to the initial stability is also of interest. Based on knowledge of the compressive behaviour of bone tissue, this thesis proposes a mathematical approach as a solution for a biomechanical analysis of these parameters.

This leads to the following problem statement:

## 4.1 Problem statement:

*How can the initial stability of the stem in various preconditions of the host bone be analysed by mathematical modelling, and which parameters are crucial for a successful result?*

# Part II

# Problem solution

CHAPTER

# 5 Modelling methods

This chapter is concerned with the mechanical behaviour of bone tissue and deriving a mathematical expression for analysing and describing the changing behaviour in different relative densities. The geometry and the geometric constrains for creating the models are also presented.

As described in the problem analysis the anatomical and biomechanical condition of bone tissue such as yield strength and elastic modulus, varies according to the individual patient. The conditions of the host bone correlated with the size of the stem are challenging and crucial for obtaining initial stability and thereby a successful result. This is essential for bone ingrowth in the surface of the prosthesis which ensures fast recovery of the patient and long term fixation.[Søren Kold and Søballe, 2004]
Since there is very sparse scientific research on that area, a mathematical approach has been chosen to analyse the influence of different preconditions of the host bone on the initial stability. The initial stability is evaluated from the calculated pull-out force of the stem from the bone.

In order to understand the mechanism and physical effect of the problem in a controlled way, an analytical model is created. This method is based on a simplified model, in this case a model of the stem inserted into metaphysial bone, to analyse the compressive behaviour of bone tissue and predict a results of the initial stability in various bone condition in a closed-form solution. This can provide qualitative information on issues such as the relations between the pull-out force and various parameters such as initial density, the angle of the stem, degree of bone compaction, and the friction between the stem and bone. The analytical model is based on rotational symmetry, so the stability regarding moment loading can not be estimated without further development of the model.

As the analytical model is limited to a simplified version of the problem, and only a guideline of the behaviour, the next step is to create a numerical model. This method allows solving more complex problems and provides the ability to analyse the model behaviour over time. A numerical method allowing this is the Finite Element (FE) method. This methods divides the complex 3D problem into a finite number of elements which are used to interpolate the displacement field.

As the FE is a numerical modelling method, the validity is not very high when standing alone. Hence, the results from the analytical model are used as a basis for creating the FE model and for validating the output in order to ensure that the results from the FE model are proper and follows the correct behaviour. The Finite element software used is LS-DYNA.

## 5.1 Mechanical behaviour of trabecular bone

In order to analyse the initial stability and simulate the compaction process, the mechanical properties of the materials in the model are needed. As described previously, the metaphysis is composed by compact bone and trabecular bone. The stem used during the compaction are titanium with a smooth surface. The values which defines the material properties are listed in table 5.1, which are Young's modulus [E], Poisson ratio [$\upsilon$] and density [$\rho$].

| | E [GPa] | $\nu$ | $\rho$ |
|---|---|---|---|
| Compact bone | $18.6^*$ | $0.3^\triangle$ | 1817 kg*m$^{-3}$ * |
| Trabecular bone | $10.4^*$ | 0.3 $^\triangle$ | 1764 kg*m$^{-3}$ * |
| Prosthesis | $110^\triangle$ | $0.3^\triangle$ | - |

***Table 5.1.*** Table showing the properties to describe the behaviour of the materials used in the models. $*$ [Ashman and Turner, 1993], $\triangle$ [Iain Spears and Hille, 1998].

These values are only valid in the linear elastic domain. The elastic parameters of the trabecular bone is not of high importance in the current context, as a very severe compaction takes place before reaching the final fixation of the stem, which is why further analysis of the behaviour is necessary.

As the bone tissue is anisotropic, the mechanical behaviour is different in the axial direction and longitudinal direction. It is also different when exposed to compressive and tensile stresses. Figure 5.1 illustrates the different behaviour during compression and tensile for compact bone, of which $*$ illustrates the behaviour in the longitudinal direction. The initial behaviour is linear elastic in both directions, but the bone tissue breaks earlier in the axial direction in both compression and tension. It can also be seen that the compact bone is elastic in a longer period during compression, compared with tensile.[Ashby and Gibson, 1999][Gibson, 1985]

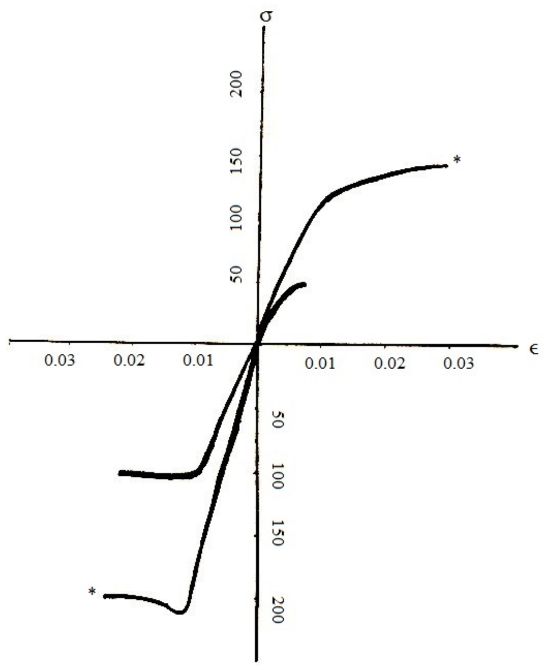


***Figure 5.1.*** Illustration based on [Ashby and Gibson, 1999][Gibson, 1985], which shows the relation between the compressive and tensile stresses $[MN/m^2]$ in compact bone. $*$ indicates the longitudinal direction, and the other illustrates the axial direction.

The tensile strength of compact bone in the longitudinal direction is approximate 50 MPa, which sets a limit to the pressure which can be achieved when compacting the trabecular bone. A too high pressure will lead to fracture of the compact bone. The mechanical behaviour of trabecular bone differs from the compact bone, because the difference in strength of the different tissue. The tensile behaviour for the trabecular bone with a relative density $\rho_r = 0.2$ is illustrated in figure 5.2. It can be seen that the bone cells during tensile stress goes from elastic to plastic deformation between 1-2 % strain, after which the decent of the curve is steep caused by damage and break of the bone cells.[Ashby and Gibson, 1999][Gibson, 1985]

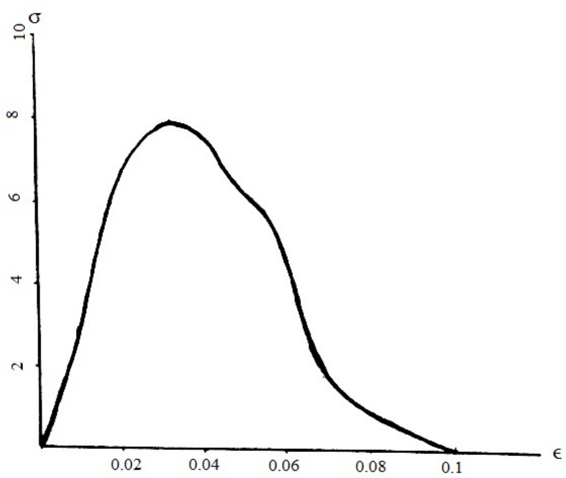


***Figure 5.2.*** Illustration based on [Ashby and Gibson, 1999][Gibson, 1985], which shows the behaviour of trabecular bone exposed to tensile stresses $[MN/m^2]$.

Low density trabecular bone has a limited capability to carry tensile loads. Figure 5.2 illustrates that the limit is 8 MPa. As for the compact bone, the compressive stresses are higher than the tensile stresses before the bone cells starts to deform plastically and collapses. The relationship between the compressive behaviour and three different relative start densities $\rho_r = 0.3, \rho_r = 0.4, and \rho_r = 0.5$ are illustrated in figure 5.3.[Ashby and Gibson, 1999][Gibson, 1985]

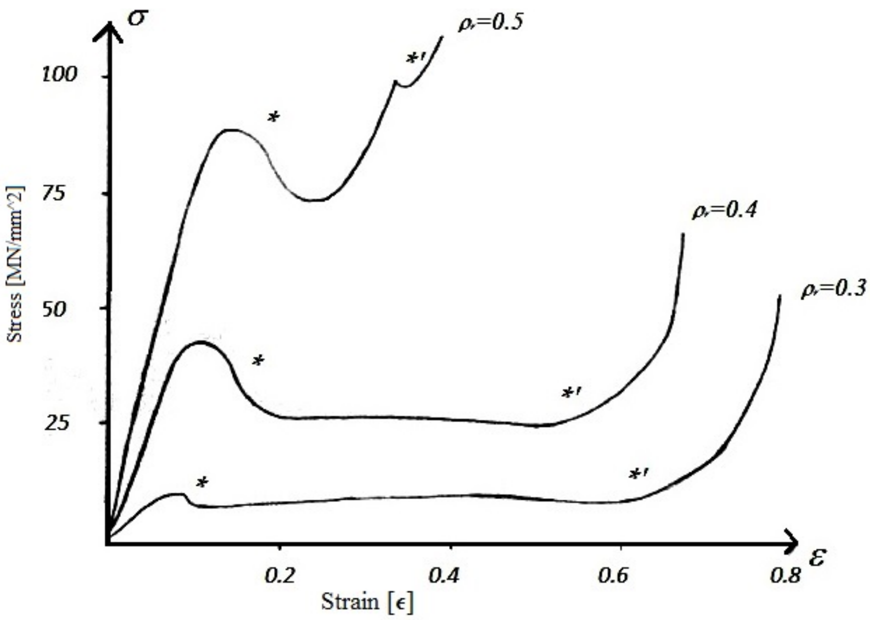


***Figure 5.3.*** Illustration based on [Ashby and Gibson, 1999][Gibson, 1985], which shows the relation between the compressive stress and engineering strain in trabecular bone with different densities.

Figure 5.3 shows the behaviour when the trabecular bone is exposed to a compressive load. It shows that the behaviour is different depending on the relative density, and that the loading modulus changes during compressive strain. The curves can roughly be divided into three different parts, of which the initial is elastic and tends to a flat plateau where the bone is compacted. This is followed by a steep ascent where densification occurs. This is when all the bone cells are collapsed, and the curve tends asymptotic against the modulus for total compact bone. The $*$ illustrates when the tissue is no longer elastic and plastic collapse occurs, and the $*'$ illustrates when the tissue becomes dense and no longer posses porous behaviour.[Ashby and Gibson, 1999][Gibson, 1985] The tangential slope in the initial part of the curves should be equal to the elastic modulus, but the modulus stated in [Ashby and Gibson, 1999] does not seem to correlate with the start slope of the curves illustrated in figure 5.3.

As it can be seen that the modulus changes during compressive stresses, an expression to describe the behaviour is sought. As the variation of the relative density is significant from patient to patient, different relative densities are examined. The relative density in trabecular bone tissue $\rho_r$ is ranged from 0.07-0.7, but it is assumed that the lowest relative density in the femoral head is > 0.2, due to the different amount of load transmissions, which leads to a higher bone density. [Ashby and Gibson, 1999][Gibson, 1985] In order to derive such expression, some assumptions regarding the mechanical behaviour have been made.

### 5.1.1 Mechanical assumptions

There is a high variability of the mechanical behaviour in bone tissue, which makes it difficult to predict the true process of the bone compaction and thereby the initial stability. In order to simplify the mathematical models and the corresponding calculations for the analytic model some assumptions regarding material properties have been made, which are described below.

The bone tissue for both trabecular- and compact bone are anisotropic which means that the mechanical behaviour depends on the direction and can be different when measured along different axis.[Ashby and Gibson, 1999] When the bone is compacted, it is exposed to a radial pressure but also an axial pressure caused by the conical angle of the stem. In the analytical model, isotropic material properties are assigned to the bone tissue resulting in identical properties regardless of the direction.

Furthermore as described in section 2.3, the density of trabecular bone varies according to several factors.[Ashby and Gibson, 1999] In order to describe the material behaviour in different densities with a specific tangent modulus, a preliminary interpretation of the stress-strain relation is made in the following section.

## 5.2 Compressive behaviour of bone tissue

When applying a force to the bone tissue a deformation will occur. This deformation is characterised by strains, of which a change in length is the normal strain and a change in angles is shear strain. The total average strain can be calculated by equation (5.1).

$$\varepsilon_{av} = \frac{\Delta L}{L_0} \tag{5.1}$$

In order to analyse the process of bone compaction and the relation between the stress and strain in the trabecular bone, a mathematical expression based on figure 5.3 is fitted for different densities to reach a similar behaviour. This can be used for finding the changing modulus when the bone tissue is exposed to a changing compressive strain. It has been chosen to utilize the engineering strain to characterize the deformation.

### 5.2.1 Derivation of an expression for the compressive behaviour

Different points on figure 5.3 are measured and a $3^{rd}$ order polynomial is found by curve fitting in order to obtain a smooth function that fits the points approximately with a number of constrains which will be described below. The curve fitting will be based an a smooth function, as the function is intended to approximately fit the data points. The choice of a $3^{rd}$ order polynomial is based on the shape, its ability to provide a smooth curve and to avoid over fitting. The curves describes the compressive behaviour with a mathematical expression for each case in the form of equation (5.2).

$$f(x) = a + bx + cx^2 + dx^3 \tag{5.2}$$

Equation (5.2) can be rewritten as equation (5.3), which is an expression for the nominal compressive stress, and the formula used for deriving the compressive behaviour.

$$\sigma_c = a + b\varepsilon_c + c\varepsilon_c^2 + d\varepsilon_c^3 \tag{5.3}$$

As [Ashby and Gibson, 1999] only illustrates the behaviour for $\rho_r = 0.3, \rho_r = 0.4 and, \rho_r = 0.5$, the tendency in the coefficients for each curve are used to predict the behaviour for $\rho_r = 0.2, and \rho_r = 0.6$ to obtain a wider spectra of preconditions. These are conducted based on linear extrapolation. This method is used to obtain a larger amount of data based on the tendency and correlation of existing data. Since it is a prediction, its accuracy is limited, but it provides an indication of the tendency of the compressive behaviour when dealing with a broader spectra of relative densities, and thereby an indication of the major influence the relative density have on the final result of the surgical procedure.

It is assumed that the compression stresses are increasing as a function of the straining, which means that there should be no negative slopes present on the curves, $E_{tan} > 0$. It is also assumed that the strains are linear and the bone is not expanded axial, which means that the relative density at 100 % compaction is $\rho_r = 1$, where the modulus goes asymptotic towards the modulus for compact bone. Normally bone with a $\rho_r > 0.7$ is considered compact bone, so the derived expression should be considered only phenomenological behaviour, which may differ quite a lot from the physical behaviour.

It is also assumed that [Ashby and Gibson, 1999] has calculated the final strain $\varepsilon_c$ at 100 % compaction at each density by equation (5.4), since the strains are positive in the figure. Equation (5.4) will also be used to calculate the ideal maximum strain, of which the curves are forced analytical to end up at. This will be used as the end condition for each curve.

$$\varepsilon_c = -\frac{\Delta L}{L_0} \tag{5.4}$$

With these assumptions and the knowledge about the final strain, curves for the different densities can be generated from the points measured in figure 5.3, which are illustrated in figure 5.4. It should be noted that the end situations of the curves is not consistent with figure 5.3 as the final compressive strain has been calculated as $\varepsilon_c = 1 - \rho_r$. E.g. in figure 5.3 a strain of almost 0.8 is reached for $\rho_r = 0.3$, of which the final strain in this case the strain will be 0.7 for $\rho_r = 0.3$.

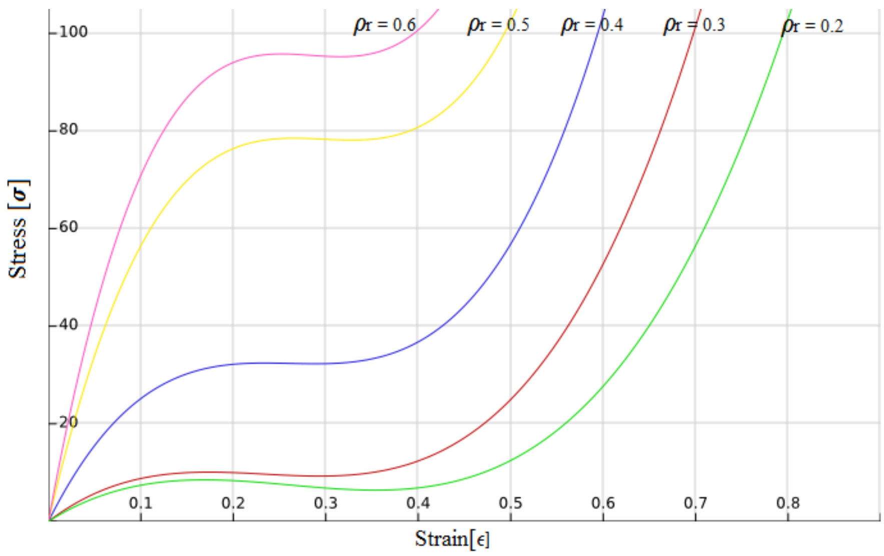


***Figure 5.4.*** Curve fitting based on [Ashby and Gibson, 1999] graph of the stress strain relation of trabecular bone with different relative densities, to describe the compressive behaviour.

These curves illustrates the stress strain relation, which can be used to identify the changing compressive modulus when dealing with different relative bone densities. As the curves from [Ashby and Gibson, 1999], the tangential slope in the initial part of the curves is not equal to the modulus stated for trabecular bone, but it is accepted, since its influence on the pressure calculations is limited. Because of the choice of fitting the expression with a $3^{rd}$ order polynomial, a negative slope is present in all curves where the tissue goes from elastic to plastic.

The behaviour of the curves is reasonable when comparing with figure 5.3, where the initial behaviour is almost linear and tends to a flat plateau followed by a steep ascent where the bone tissue goes from compact to dense. The plateau is slightly decreasing which obviously is inaccurate, but a consequence of the choice of fitting the curves in accordance to a $3^{rd}$ polynomial.

By finding the slope of the tangent in a certain point, the modulus $E_{tan}$ can be calculated. The changing modulus is illustrated in figure 5.5, where the mathematical expression found for each relative density is differentiated.

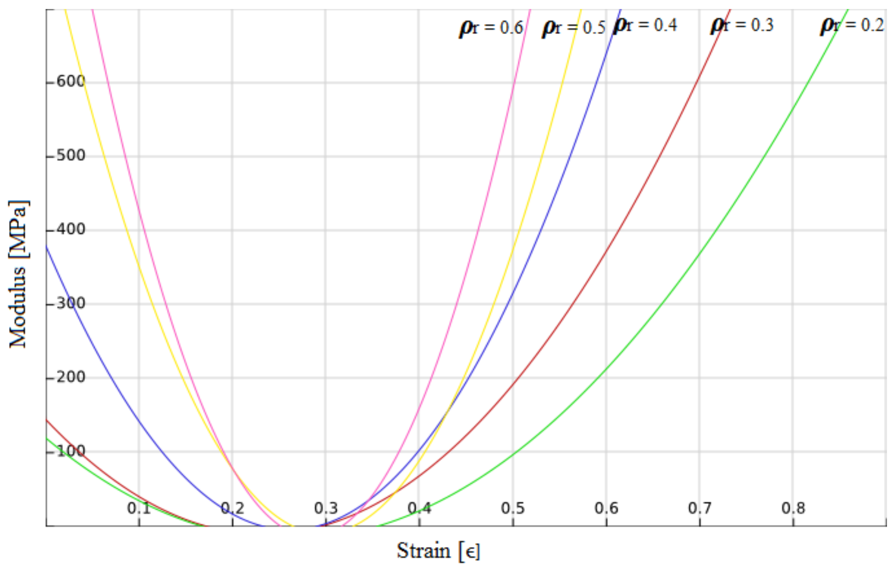


***Figure 5.5.*** Curves showing the changing tangent modulus of trabecular bone when exposed to a compressive strain. Periods with negative slopes is present with the curves in figure 5.4, which gives a negative modulus.

It is seen that the modulus is decreasing during the deformation and becomes zero when plastic collapse in the tissue occurs. Because of a slightly negative slope in figure 5.4, the modulus will be negative, which is intended to be horizontal in the stress strain diagram in figure 5.4, caused by the fitting method.

This behaviour would cause problems if the deformation is force-controlled, however, in the analytical model the response is calculated assuming a displacement-controlled process, whereby snap-through effects are avoided. In the FE domain, such a material behaviour would result in an unstable dynamic response, which can be controlled by ensuring a stiffening response, e.g. by taking viscous effect into account or including the visco-plastic deformation.

CHAPTER

# 6 Analytical model

In order to characteristic the initial stability of the prosthesis, the pull-out force of the stem from bone is estimated. This force is depending on several parameters such as the tangent modulus, unloading modulus, geometric properties, friction between bone and stem, and relative density. The analytical model is a simplified rotationally symmetric model of the bone and stem in order to analyse the initial stability, pull-out force and provide an understanding of the mechanical behaviour of the process with different preconditions in the host bone. This chapter will present a model of the analytical geometric structure and the methods for estimating the pull-out force.

## 6.1 Geometric interpretations

It is assumed that the stem is cylindrical, with an increasing radius along the z axis caused by the conical geometry. The geometry of the metaphysis is also assumed to be cylindrical, and the anatomical dimensions are approximated to values from a x-ray obtained from a femur with a 24 mm Primoris stem inserted, which can be found in appendix A. The frontal radius of the metaphysis is measured to be 20 mm, and the thickness of the compact bone to be 3.3 mm. A schematic illustration of the insertion process and the interference between the stem and a cylindrical model of the bone are illustrated in figure 6.1s.

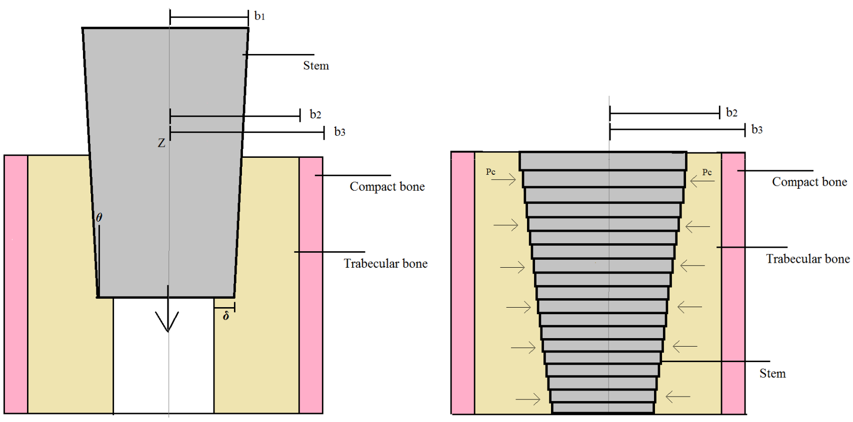


***Figure 6.1.*** Illustration of the geometry before and after insertion, divided sectionally in the z-direction.

In order to calculate the contact pressure between the bone and the stem, and thereby analyse the mechanics of a general interference fit, the conical stem is divided into a series of straight cylinders with changing radius, as illustrated to the right in figure 6.1. This provides a basic interpretation of the mechanical behaviour during the insertion process.

In the real process, the initial tools "rasps" the bone to create the hole before the compaction process. This results in an increased amount of trabecular bone in the bottom, which is not taken into account in this model.

In the presented model, the deformation of the trabecular bone is assumed to start from a cylinder and end as a cone caused by the conical geometry of the stem. A single slice will be analysed in order to find the plane stresses and thereby derive an expression for the contact pressure as illustrated in figure 6.2. The slice is assumed to be in plane stress. (When taking the compression into account it is also assumed that it maintain it's thickness.)

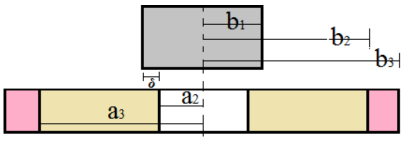


***Figure 6.2.*** Illustration of a slice of the model denoted with designations for the dimensions to be used when calculating the pull-out force.

Before the prosthesis is inserted, the trabecular bone is compacted with increasing sizes of smooth tapered stems of which the top diameter ranges from $D = 18mm$ to $D = 24mm$, which corresponds to the size of the prosthesis. The degree of compaction is described as the radial displacement $\delta$ = b1 - a2. The conical geometry results in a varying contact pressure between the stem and bone.

### 6.1.1 Contact pressure between stem and bone

Each part of the model is exposed to an inner pressure $P_i$ and an outer pressure $P_o$ when the stem is inserted into the bone because of the initial compaction as illustrated in figure 6.3. [Dally and Riley, 1987] I illustrates the pressure on the compact bone, II illustrates the pressure of the trabecular bone and III illustrates the pressure on the stem.

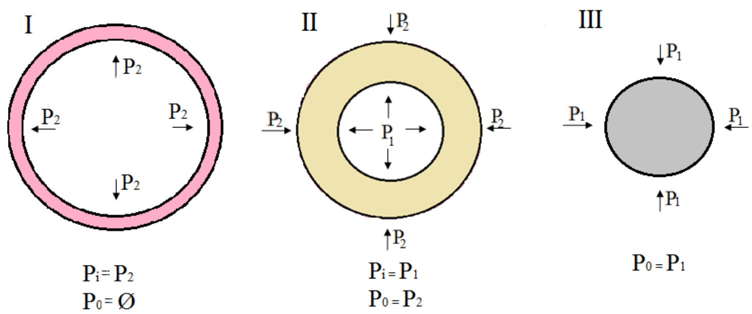


***Figure 6.3.*** The geometry of a slice of the model when the stem is inserted into the methaphysis, where each part is exposed to an inner and outer pressure.

This loading is quite similar to press fitting two rings on a shaft. Here the inner pressure $P_i$ and outer pressure $P_o$ can be obtained by using the equation for the radial displacement $U$, of which equation (6.1) is for the inner ring of the trabecular bone and equation (6.2) is for the inner ring of the compact bone, of which the outer pressure is zero. [Dally and Riley, 1987] The notation follows figure 6.2. E is Young's modulus and $\nu$ is the Poisson ratio.[Dally and Riley, 1987]

$$U(b1) = \frac{1}{E_t}\frac{(-b1^2 * b2^2 * (P_o - P_i))}{2b^2 - b1^2 * r} * (1+\nu_t) + \frac{P_i * b1^2 - P_o * b2^2}{b2^2 - b1^2} * (1-\nu_t) * r \tag{6.1}$$

$$U(b2) = \frac{b2^2 * P_i}{E_c * r * (b3^2 - b2^2)} * ((1+\nu_c) * b3^2 + (1-\nu_c) * r^2) \tag{6.2}$$

As the changing displacement is known, these equations provides a method for calculating the changing pressure when the angle of the stem is not taken into account. The equations are however only valid for linear elastic materials. To extent these expressions to be valid when finding the contact pressure, the expressions found in subsection 5.2.1 for the changing compressive behaviour is taken into account.

As these equations are valid for linear elastic problems. The use may include some discrepancy from the non-linear behaviour of the bone tissue and the use of engineering strain.

## 6.2 Process of bone compaction

To estimate the contact pressure between the stem and bone, the average volumetric strain is found, as a function of the increased radial displacement. The radius of the stem is set to start at 9 mm (identical to the start radius of the hole in the bone), in order to analyse the compaction process. The volumetric strain can be calculated by using equation (6.3), of which x is the radius of the stem at the actual height. The compact bone is set to be rigid and a potential circumferential variation is not taken into account.

$$\varepsilon_c(x) = 1 - \frac{b2^2 - x^2}{b2^2 - b1^2} \tag{6.3}$$

Using the expressions found for the different relative densities and to utilize these, a stepwise method may be used to estimate the contact pressure, and the radial pressure can be calculated by equation (6.4), which is more consistent with the method [Ashby and Gibson, 1999] used. However the large straining will also lead to significant deviations.

$$P = a + b * \varepsilon_c(x) + c * \varepsilon_c(x)^2 + d * \varepsilon_c(x)^3 \tag{6.4}$$

The coefficients varies according to the density of interest and $\varepsilon_c$ corresponds directly to the volumetric strain. This results in an expression for the contact pressure for a single slice.

### 6.2.1 Pull-out force

The pressure for each slice is assumed to interact in correlation with increased radius of the stem, such that the pressure calculated interacts normal to the stem surface. In order to calculate the pull-out force, the contact pressure for the slice with changing conical radius b1(z), is obtained from the entire model. The contact force N is thereby found by integrating the contact pressure by equation (6.5), between the prosthesis and the trabecular bone over the contact area of the prosthesis.[Bozkaya and Muftu, 2002] An illustration of the process can be seen in figure 6.4.

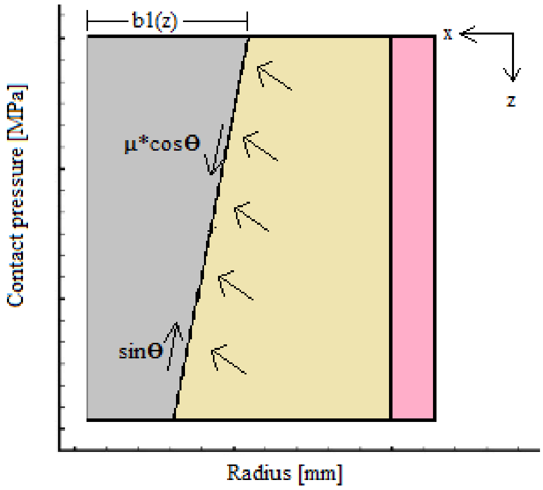


***Figure 6.4.*** The geometry for finding the contact pressure and thereby the contact force.

$$N = 2\pi \int_0^{H*cos\theta} b1(z) * P dx \tag{6.5}$$

The total pull-out force can then be calculated by equation (6.6).[Bozkaya and Muftu, 2002]

$$F_p = -N * (sin\theta - \mu * cos\theta) \tag{6.6}$$

Since the equation for finding the pressure is a function of the height H of the stem, the equation for the pull out force can be written as equation (6.7), which results in integrating according to the increased radius instead of the height H. As $\theta$ is pretty low, the error evidently introduced is expected to be very small.

$$F_p = -2\pi \int_9^x b1(z) * P * (sin\theta - \mu * cos\theta) * \frac{b1(z) - x}{H} dx \qquad (6.7)$$

$P * sin(\theta)$ is the pressure which pushes the stem up generated by the conical geometry, and $P * \mu * cos\theta$ is the value holding the stem down caused by the friction between bone and metal.

This provides the basis for the analytical model, which gives an understanding of the mechanical behaviour of the bone tissue when inserting a femoral stem. The model can be used for analysing different preconditions of the host bone, of which parameters such as the relative density, conical angle of the stem and frictions between bone and stem is of interest. It can also be used to indicate the preconditions for obtaining the best initial stability.

CHAPTER

# 7 Analytic parameter study of preconditions

The anatomical and biomechanical conditions varies according to the patient, and it is known that parameters such as the relative density of the bone tissue, the contact pressure between the bone and stem, radius of trabecular bone and the friction coefficient between bone and stem, may influence the pull-out force. These parameters are investigated in order to provide knowledge of which preconditions will lead to a successful result. In this chapter a parameter study is conducted, where the influence of the different preconditions of the host bone are examined. At first the contact pressure between the bone and stem is found for different relative densities, along with an indication of the amount of bone compaction required for obtaining maximum contact pressure. Afterwards the effect of different conical angles of the stem, in accordance to the pull-out force is examined, and at last the influence of the radius of the trabecular bone in accordance to the pull-out force is analysed.

The contact pressure and the corresponding pull out force for all parameters are calculated for the five relative densities $\rho = 0.2, \rho = 0.3, \rho = 0.4, \rho = 0.5, and \rho = 0.6$, of which the compressive behaviour previously have been investigated and described mathematically. The geometry of the model which provides the basis for all the parameter studies is illustrated in figure 7.1, of which $\mu$ is the friction coefficient, and $\theta$ is the angle of the cone. These are the parameters that leads to a geometric variation of the final result, since b1(z) and b2 is depending on the angle.

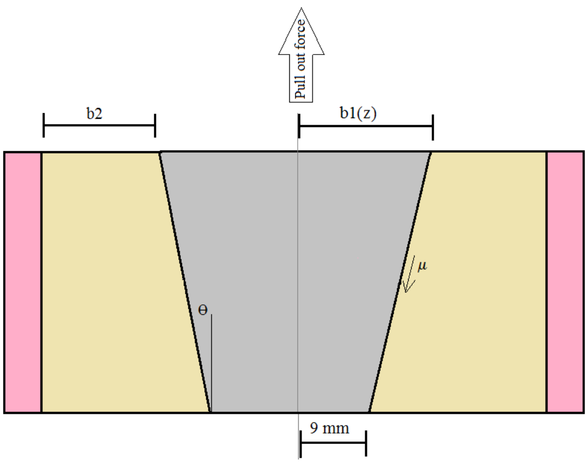


***Figure 7.1.*** Illustration of the geometric constrains used for finding the contact pressure and pull out force.

## 7.1 Contact pressure and maximum bone compaction

In this section the contact pressure between the bone and stem is presented, which is found with a fixed friction at $\mu = 0.75$ based on [Niklas B. Damm, 2015], a bone radius at 16.7 mm as illustrated in figure 7.1, and $\theta = 3.5$.

The pressure when bone tissue with different relative density is compacted with the previously described stem is found by inserting the respective variables for the corresponding relative densities into equation (7.1), which was derived in section 6.2.

$$P = a + b * \varepsilon_c(x) + c * \varepsilon_c(x)^2 + d * \varepsilon_c(x)^3 \tag{7.1}$$

The total contact pressure is found as a function of the increasing conical radius from 9 mm to b1(x)=12 mm, which is the interpretation of the real process of inserting the stem into host bone with different relative densities.

Subsequent the top diameter b1(x) is increased from 9 mm to 16 mm, to see when maximum pressure is obtained and the bone is totally compacted with $\rho_r = 1$. This provides an insight of the amount of bone compaction required as a function of the relative density in order to achieve an acceptable pressure that generates stability. This can be used for evaluating the limit for when bone compaction no longer provides a successful result.

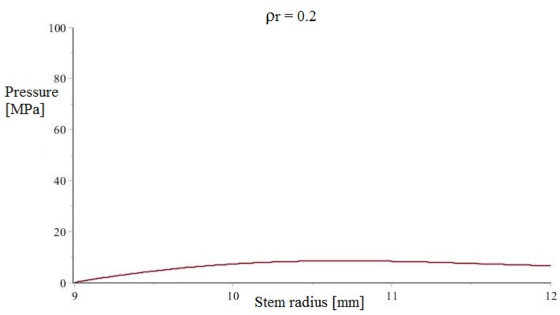


***Figure 7.2.*** The contact pressure between bone with $\rho_r = 0.2$ and the stem. 7 % compaction is obtained when the stem is inserted.

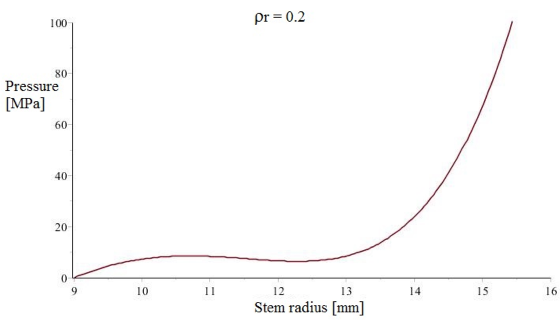


***Figure 7.3.*** The increasing stem radius as a function of contact pressure. This indicates the maximum stem radius for $\rho_r = 0.2 = 15.4$ mm when $\rho_r = 1$.

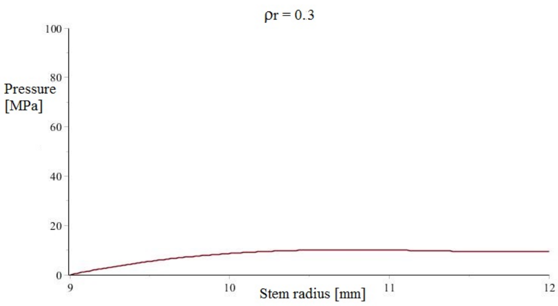


***Figure 7.4.*** The contact pressure between bone with $\rho_r$ = 0.3 and the stem. 9.5 % compaction is obtained when the stem is inserted.

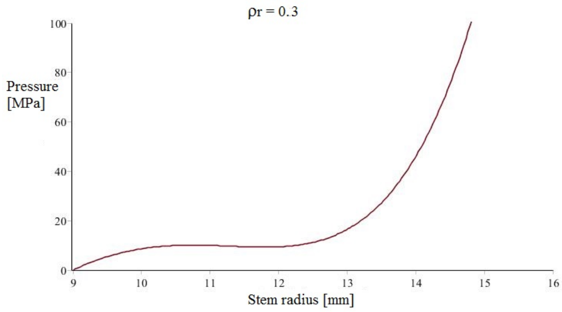


***Figure 7.5.*** The increasing stem radius as a function of contact pressure. This indicates the maximum stem radius for $\rho_r$ = 0.2 = 14.8 mm when $\rho_r$ = 1.

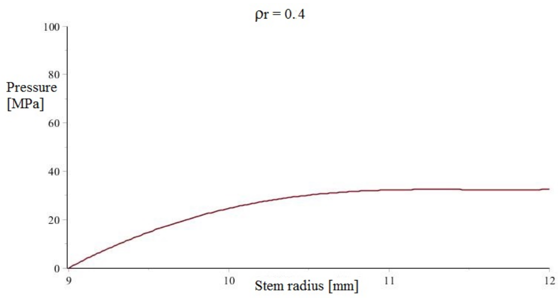


***Figure 7.6.*** The contact pressure between bone with $\rho_r$ = 0.4 and the stem. 32 % compaction is obtained when the stem is inserted.

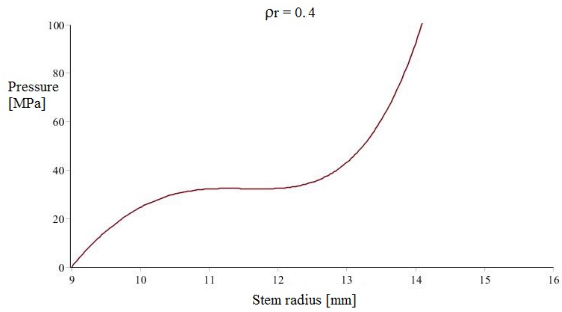


***Figure 7.7.*** The increasing stem radius as a function of contact pressure. This indicates the maximum stem radius for $\rho_r$ = 0.2 = 14.1 mm when $\rho_r$ = 1.

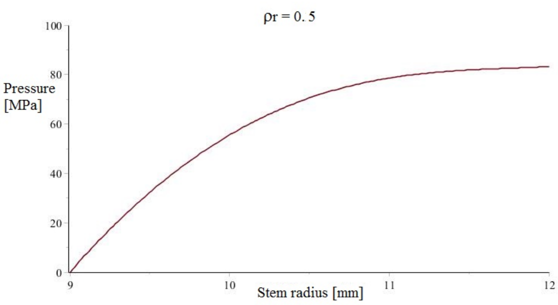


***Figure 7.8.*** The contact pressure between bone with $\rho_r$ = 0.5 and the stem. 83 % compaction is obtained when the stem is inserted.

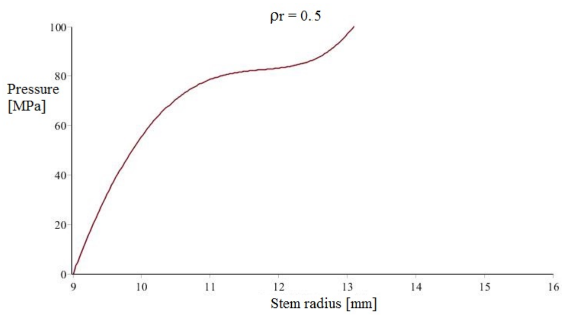


***Figure 7.9.*** The increasing stem radius as a function of contact pressure. This indicates the maximum stem radius for $\rho_r$ = 0.2 = 13.2 mm when $\rho_r$ = 1.

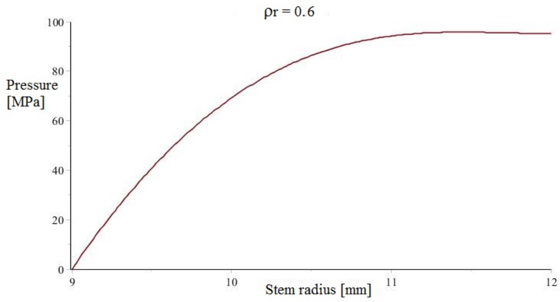


***Figure 7.10.*** The contact pressure between bone with $\rho_r$ = 0.6 and the stem. 94.7 % compaction is obtained when the stem is inserted.

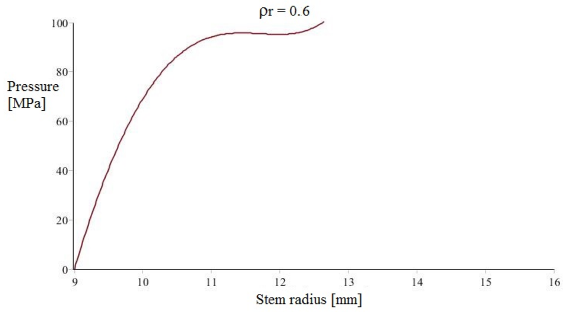


***Figure 7.11.*** The increasing stem radius as a function of contact pressure. This indicates the maximum stem radius for $\rho_r$ = 0.2 = 12.6 mm when $\rho_r = 1$.

The graphs shows a significant variation in the contact pressure between the bone and stem depending on the relative density. The lowest pressure is obtained at $\rho_r$ = 0.2, where only 7 % compaction is obtained when the stem is inserted. For the other cases the obtained compaction are respectively 9.5 % at $\rho_r$ = 0.3, 32.3 % at $\rho_r$ = 0.4, 82.7 % at $\rho_r$ = 0.5, and 94.7 % at $\rho_r = 0.6$.

Additionally the bone tissue have to be compacted 92 % in order to achieve maximum contact pressure at $\rho_r$ = 0.2, 88% at $\rho_r$ = 0.3, 84% at $\rho_r$ = 0.4, 78% at $\rho_r$ = 0.5, and 75% at $\rho_r$ = 0.6. This indicates that further compaction is necessary when $\rho_r$ decreases, in order to obtain the same pressure.

The curves in figure 7.2 and figure 7.4 contains a negative end slope which contributes with a slightly decreasing contact pressure. This effect is caused by the negative slopes found in the mathematical expression for the compressive behaviour in section 5.2, figure 5.4.

## 7.2 Effect of varying friction and angle of the stem

In order to find which stem geometriy that provides the best initial stability, different friction coefficients and different conical angles are examined. Figure 7.12 illustrates the geometric differences of the stem when changing the angle of the cone, of which the angle is controlled by the length of b1(x).

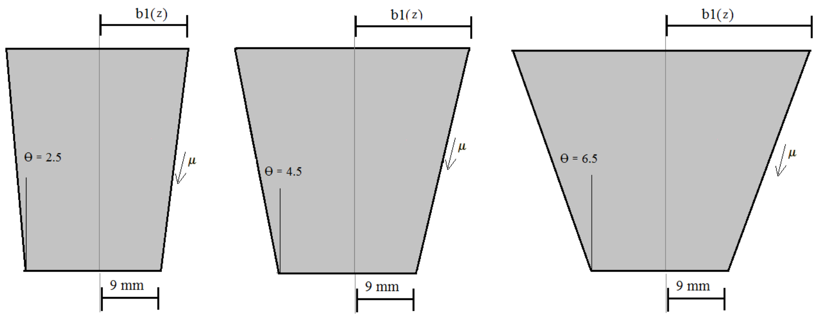


***Figure 7.12.*** Illustration of the geometric consequences when changing the cone angle of the stem.

In order to cover a broad spectre of friction coefficients, a range from 0.1 to 0.75 are investigated. These numbers are chosen based on the results from [Niklas B. Damm, 2015], who investigated the friction between different surfaces and bone.

As the true conical angle is approximately 3.5 °, which is why a spectre of angles near this value is chosen. The pull-out force is found for the different angles 2.5 °, 3.5 °, 4.5 °, 5.5 °, and 6.5 °as a function of increasing friction coefficients.

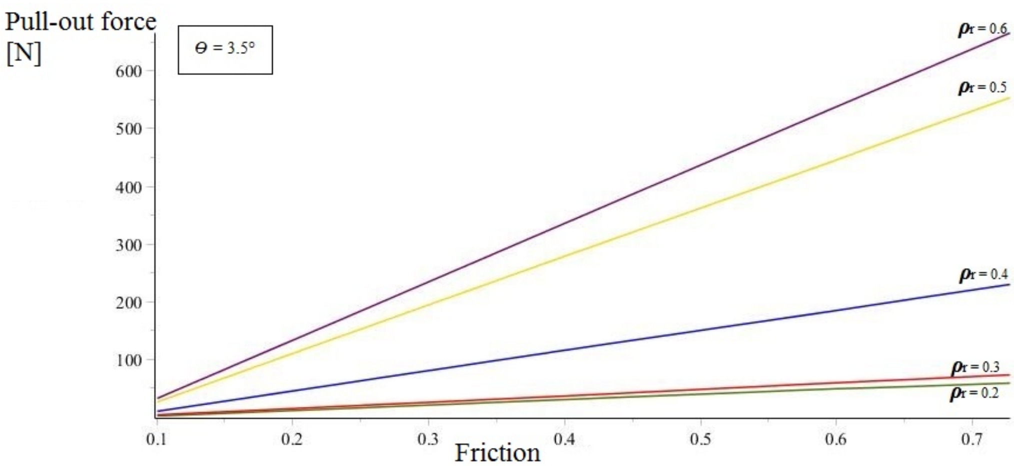


***Figure 7.13.*** The pull out force with a conical angle $\theta$ = 3.5, which is similar to original geometry, as a function of different frictions coefficients.

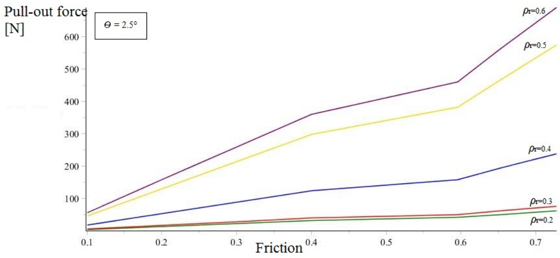


***Figure 7.14.*** The pull out force with a conical angle $\theta$ = 2.5 as a function of different frictions coefficients.

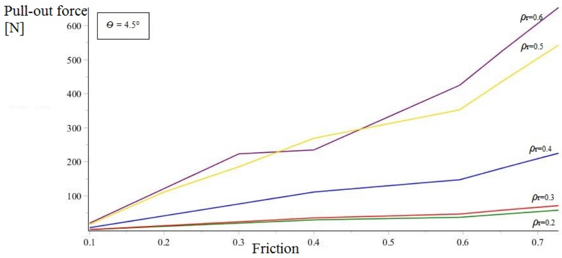


***Figure 7.15.*** The pull out force with a conical angle $\theta$ = 4.5 as a function of different frictions coefficients

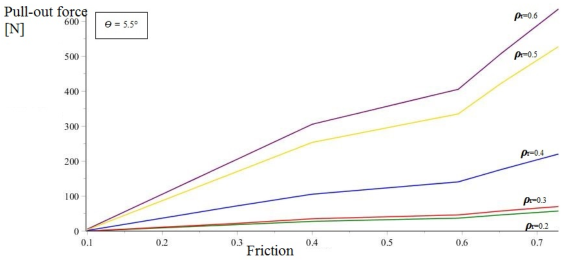


***Figure 7.16.*** The pull out force with a conical angle $\theta$ = 5.5 as a function of different frictions coefficients

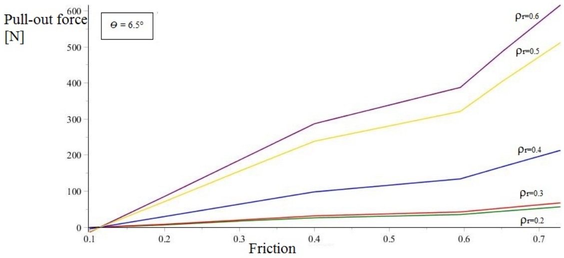


***Figure 7.17.*** The pull out force with a conical angle $\theta$ = 6.5 as a function of different frictions coefficients. Some values are negative caused by exceeds the critical angle.

It can be seen that the pull-out force for all densities are increasing as a function of the frictions coefficient. It can thereby be resolved that a higher friction coefficient provides a greater pull-out force under all circumstances, and that it have a major effect on the initial stability. The tendency of the curves is similar in all cases with an almost linear piece in the middle of all graphs which leads to a steep ascent at friction 0.6. The similar behaviour can be a consequence of the previously made assumptions for calculating the pull-out force. The linear piece can be caused by the negative slopes found for the compressive behaviour.

The angle of the conical stem is also affecting the final pull out force. It is seen that a greater angle does not provide a higher pull out force. The highest values are found with a conical angle of $\theta$ = 2.5, and the lowest with a conical angle of $\theta$ = 6.5. It is also seen that an angle of $\theta$ = 6.5 provides negative results with friction = 0.1, which means that the stem is not stuck. This is because of the cone angle exceeds the critical angle when the friction is 0.1. This is a consequence of $sin(\theta) > \mu * cos(\theta)$.

### 7.2.1 Critical angle of the stem

The critical conical angle of the stem regarding the friction coefficient can be investigated by solving equation (7.2), of which the result is illustrated in figure 7.18. This provides an interpretation of the impact that the friction has on the level of the angle, which thereby can be used to define some geometric constrains for the stem.

$$sin(\theta) - \mu * cos(\theta) = 0 \tag{7.2}$$

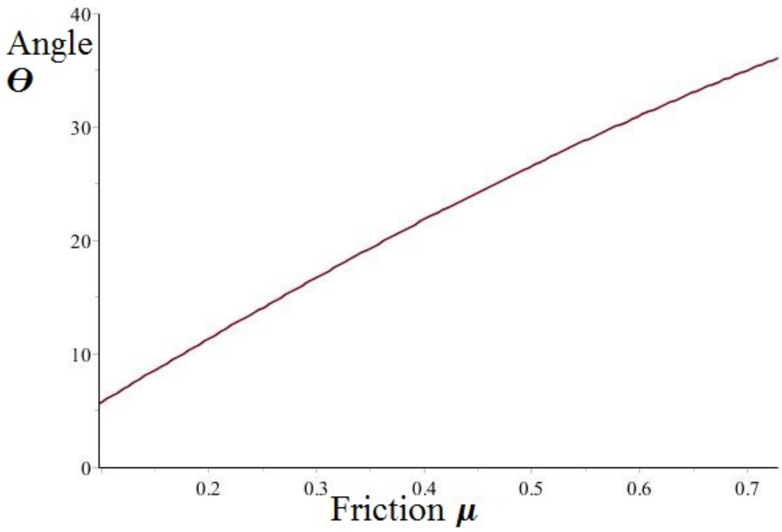


***Figure 7.18.*** Illustration of the geometric consequences when changing the conical angle of the stem.

It can be seen in figure 7.18 that the value for the critical angle increases almost linear when the friction coefficient is increased. The critical angle at $\mu$ = 0.1 is 5.8 °, which indicates the geometric constrains for the stem, as it is the lowest friction for the surgical equipment. Though the friction coefficient for the prosthesis is higher, the geometry have to comply with the geometry for the initial tools used for bone compaction. This confirms the negative values obtained in figure 7.17, as it can be seen that the critical angle for $\mu$ = 0.1 is 5.8 °, and that no contact force will exist in this case. A large friction may introduce shear failure in the bone, e.g. a friction coefficient of 0.75 may easily lead to shear stress much higher than the critical shear stress.

## 7.3 Effect of varying radius of the trabecular bone

As described earlier, the anatomy of the human metaphysis varies according to the patient. In order to investigate which effect the outer radius of the trabecular bone have on the initial stability, the pull-out force is found for different radii of the trabecular bone, with different relative densities. The radius is varied from 13.5 mm to 19.5 mm. The geometry of the stem is as shown in figure 7.1, with $\theta$ = 3.5 and b1(z) = 12 mm. This provides an interpretation of how the initial stability is affected if choosing a stem that does not correspond to the size of the trabecular bone.

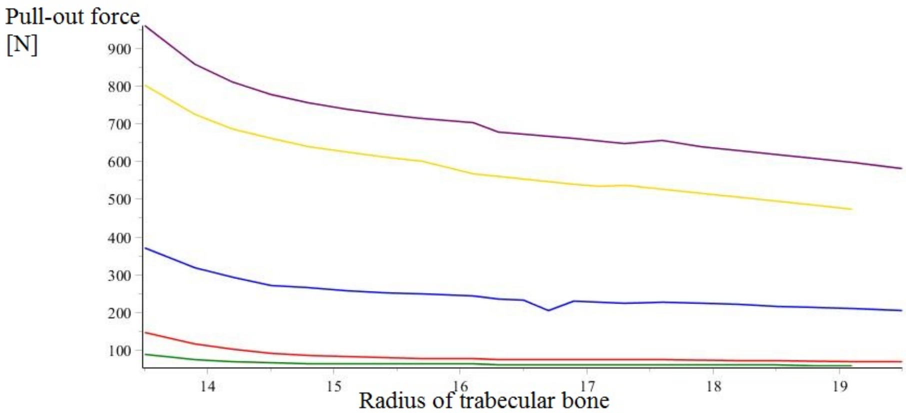


***Figure 7.19.*** The pull out force as a function of increased radius of trabecular bone for different relative densities.

It is seen in figure 7.19 that the outer radius of the trabecular bone have a significant effect on the pull out force. The effect is highest at $\rho_r = 0.5$ with a decrease at 41 % of the pull out force from the lowest radius to the highest radius. The smallest change is seen in $\rho_r = 0.2$ with a decrease at 33 %. The decrease at $\rho_r = 0.6$ is 39 %, $\rho_r = 0.4$ is 37 %, and $\rho_r = 0.3$ is 34 %. This imply that a smaller start radius of the trabecular bone results in a greater pull out force and consequently a better initial stability of the stem. This means that the size of the stem should be chosen in accordance to the amount of the trabecular bone. This can be used to provide guidance of the size of the initial hole, which in combination with b1(z) and $\rho_r$ should lead to a certain pull-out force and thereby initial stability.

An analytical model has been developed to estimate the pull-out force as a function of various parameters. A natural development would be to estimate the circumferential stress in the compact bone to investigate the correlation between pull-out force and the risk of fracture when inserting the stem. Here the stress may be estimated with an approach as in equation (6.1) and equation (6.2) for a press fit.

CHAPTER

# 8 Finite Element modelling

As the analytical model is a simple model of the problem, a FE model is created, to increase the ability to include more complex geometry and thereby more complex loadings. The results and understanding of the compaction process from the analytical model are used as basis for creating the FE model. The model is created using the Finite Element software LS-DYNA. In this chapter the theory and procedures behind FE modelling will be briefly introduced to provide an overview of the basic principles for creating a model in this domain. The approach is to work with the FE model in relation to the analytical model coupled with the point of view used to generate the curves for the compressive behaviour of trabecular bone.

## 8.1 FE theory

In order to simulate and predict the initial stability of the stem, a FE model is developed. This method is often used in order to evaluate biomechanical problems and in this case it can be used for a mechanical analysis of the initial stability. In order to validate the FE model, the prediction of the stability found analytically in chapter 5 will be used to validate the results obtained by the FE model. Emphasize is primarily to apply a qualitative response.

FE is a method for solving the partial differential equations in a complex model by dividing the model into a mesh, which is a finite number of simple elements such as triangles, quadrilaterals, tetrahedra, or hexahedra in order to obtain a numerical solution. This simplifies the geometry and makes is possible to perform calculations regarding specific physics which in this case will be a stress analysis. [Robert Cook and Plesha, 1992][Khoei, 2005]

The approach for creating the FE model is shown in figure 8.1


***Figure 8.1.*** The different steps in order to create a Finite Element model.

First the geometry of the model and the physical problem have to be described. The materials in the model are defined and assigned with the mechanical properties such as Young's modulus (E) and Poisson's ratio ($v$) for elastic problems. Then the boundary conditions are assigned, which are the constrains for the model of which the solutions to the differential equations are dependent on. These ensures that the model behaves as intended.[Robert Cook and Plesha, 1992][Khoei, 2005]

In order to divide the model into finite elements, a mesh is applied. The mesh is an approximation of the geometry, which allows global calculations. The elements in the mesh can be of different sizes and shapes, and are connected in nodes. At last the model is solved and the simple equations for each element are assembled into a larger system of equations and an approximate solution for the whole model is found based on a given input.[Robert Cook and Plesha, 1992][Khoei, 2005]

### 8.1.1 Dynamic equilibrium in FE domain

Given that a FE model is dynamic, it has to maintain a dynamic equilibrium. This means that the internal- and external forces in the system have to be in balance, which is described by Newton's 2. law. The dynamic equilibrium for linear elastic problems is found by equation (8.1).[Robert Cook and Plesha, 1992][Khoei, 2005]

$$[M] * \{a\} + [C] * \{v\} + [K] * \{x\} = \{F_{ext}\} \tag{8.1}$$

In which [M] is mass matrix, *{a}* is acceleration vector, [C] is external damping matrix, *{v}* is velocity vector, [K] is the stiffness matrix and *{x}* is the displacement vector, which combined have to be equal to the external force $\{F_{ext}\}$.[Robert Cook and Plesha, 1992][Khoei, 2005]

But as the bone tissue is non-linear, the expression for finding the equilibrium is defined as equation (8.2),of which $F_{int}$ is the internal force vector.[Robert Cook and Plesha, 1992][Khoei, 2005]

$$[M] * \{a\} + [C] * \{v\} + \{F_{int}\} = \{F_{ext}\} \tag{8.2}$$

To develop a model for analysing the compaction problem, this equation have to be solved. It is important that the equilibrium conditions between the forces in the model are satisfied. The following section will provide an insight of how to obtain the discretized equations to be solved for linear elastic problems.

### 8.1.2 Potential energy in the model

The approach when working with FE modelling and knowing the formula for solving the displacement in one element, is to integrate for the whole geometry $\Omega$. This is done by equation (8.3) for the potential energy $\Pi_p$.[Robert Cook and Plesha, 1992][Khoei, 2005]

$$\Pi_p = \int_\Omega \frac{1}{2}\{\varepsilon\}^T * [E] * \{\varepsilon\} d\Omega - \int_\Omega \{u\}^T * \{\text{F}\} d\Omega - \int_S \{u\}^T * \{\Phi\} dS - \{D\}^T * \{P\} \tag{8.3}$$

Where:
*{u}* = Displacement field
$\{\varepsilon\}$ = Strain field
$[E]$ = Matrix for material properties
$\{F\}$ = Body force
$\Phi$ = Surface tractions
$\{D\}$ = Nodal degrees of freedom (d.o.f)
$\{P\}$ = Applied load to d.o.f. by external agencies
S = Surface area

The displacement field is found by multiplying the element nodal d.o.f. $d$ with the shape function matrix [N] by equation (8.4). [N] is an approximation which characterises the material properties of the elements in the mesh.[Robert Cook and Plesha, 1992][Khoei, 2005]

$$\{u\} = [N] * \{d\} \tag{8.4}$$

When knowing the displacement field, the strain can thereby be found by multiplying with the differential matrix $[\delta]$, as written in equation (8.5).[Robert Cook and Plesha, 1992][Khoei, 2005]

$$\{\epsilon\} = [\delta] * \{u\} \tag{8.5}$$

The stiffness matrix for each element is found by equation (8.6).[Robert Cook and Plesha, 1992][Khoei, 2005]

$$[k] = \int_{\Omega e} [B]^T * [E] * [B] d\Omega \tag{8.6}$$

$\Pi_p$ can now be written as a function of the global nodal displacement $\{D\}$ by equation (8.7).

$$\Pi_p = \frac{1}{2} * \{\text{D}\}^T * [K] * \{\text{D}\} - \{\text{D}\}^T * \{\text{R}\} \tag{8.7}$$

When this is set to be equal to the nodal equilibrium {0}, the formula for finding the potential energy in the displacement field is equation (8.8).[Robert Cook and Plesha, 1992][Khoei, 2005]

$$\{\frac{\delta \Pi_p}{\delta D}\} = \{0\}, \quad \longrightarrow \quad [K]\{D\} = R \tag{8.8}$$

The above mentioned expressions are valid when the material is linear elastic. These are used for deriving the expressions for describing the material when the mechanical behaviour is no longer linear elastic. When assuming the external damping is not of importance, equation (8.2) can be written as equation (8.9), which is valid for non-linear elastic problems.[Robert Cook and Plesha, 1992][Khoei, 2005]

$$[M] * \{a\} + \{F_{int}\} = \{F_{ext}\} \tag{8.9}$$

These equations provides the basis for solving a model in the FE domain for non-linear elastic problems. The next step is to choose the model parameters and verify that the material behaviour are in accordance with the theory. The total potential should be stationary, which for linear elastic problems can be ensured by having the gradient $\{\frac{\delta \Pi_p}{\delta D}\} = \{0\}$

### 8.1.3 Geometry update through FE loop

As mentioned previously, the method used in FE modelling is by updating the model incrementally in time. The start conditions for the model is stated in equation (8.10), where t is the time, $X_\alpha$ is the initial coordinates, and $x_i$ is the new position. [LSTC, 2007]

$$x_i = x_i(X_\alpha, t) \tag{8.10}$$

In order to update the geometry to the new coordinates, the velocity {v} is found and added to the previous geometry in equation (8.11).[LSTC, 2007]

$$u^{n+1} = u^n + v^{n+\frac{1}{2}} * \Delta t^{n+1/2} \tag{8.11}$$

This results in equation (8.12) for updating the initial geometry.[LSTC, 2007]

$$x^{n+1} = x^0 + u^{n+1} \tag{8.12}$$

The change in stress when working with elastic-plastic material in the model is found by equation (8.13), where the new value in time is found by the previously value plus the time derivative of the stress, multiplied with the time step. [LSTC, 2007]

$$\sigma_{ij}(t + \Delta t) = \sigma_{ij}(t) + \sigma'_{ij}\Delta t \tag{8.13}$$

In order to perform stepwise calculations for predicting and updating each incremental deformation, explicit time integration is used. It is assumed that the values for the displacement, velocity internal- and external forces to time $t_n$ are known, and thereby the values for the next time step $t_{n+1} = t_n + \Delta$t can be found by using Taylor series in equation (8.14).[Robert Cook and Plesha, 1992][Khoei, 2005]

$$\{x_{n+1}\} = \Delta t^2 * [M]^{-1} * (\{F_{ext,n}\} - \{F_{int,n}\}) + 2 * \{x_n\} - \{x_{n-1}\} \tag{8.14}$$

Ensuring [M] being diagonal makes it possible to explicit update $\{x_{n+1}\}$. In similar ways the stepwise calculations for predicting and updating the strains in the model from time n to time n+1 can be found by equation (8.15).[Robert Cook and Plesha, 1992][Khoei, 2005]

$$\varepsilon_{ij} = \varepsilon_{ij}^{n} + \rho_{ij}^{n} + \varepsilon_{ij}'^{n+1/2} * \Delta t^{n+1/2} \tag{8.15}$$

Of which the strain rate tensor $\varepsilon'_{ij}$ is found by equation (8.16), where v is the velocity vector.[Robert Cook and Plesha, 1992][Khoei, 2005]

$$\varepsilon'_{ij} = \frac{1}{2} * (\frac{\delta v_i}{\delta x_j} + \frac{\delta v_j}{\delta x_i}) \tag{8.16}$$

This is repeated for each incremental deformation from $t = 0$ to the final state to find a continuous stress strain update of the geometry.[Robert Cook and Plesha, 1992][Khoei, 2005]

## 8.2 Creating the model in LS-DYNA

When building a FE model in LS-DYNA, different prescribed material models can be applied depending on which behaviour is best suited for the material of interest. These are designed to simulate the unique behaviour of a specific material. The material model is chosen based on the previously found behaviour of bone tissue. In this case material model MAT_005 contains a similar compressive behaviour as the behaviour found for trabecular bone. This model is often used for low density foams with an open cell structure, which is similar to the bone structure with low densities.

The logarithmic volumetric strain as a function of pressure during compression of this material model is illustrated in figure 8.2, and compared with figure 5.3 and figure 5.4, the curve is initiating linear until the cell structure is collapsing and finally with a steep slope caused by densification. Unloading follows linear elastic behaviour. [LSTC, 2007]

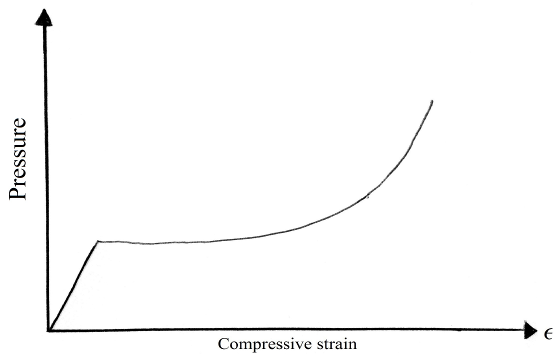


***Figure 8.2.*** Pressure as a function of logarithmic volumetric strain for the material model MAT-005 in LS-DYNA, which contains the same structure as the behaviour for trabecular bone.

In order to specify the material model to the behaviour of bone, different parameters are assigned such as the density, shear modulus and pressure cut off for the final elastic modulus. Pressure cut set a limit to the hydrostatic stress, of which the material can carry. Then up to 10 defined points can be assigned to model the curve in order to apply the correct behaviour. [LSTC, 2007] The values for these parameters are determined based on the analytical model.

In order to verify that the chosen input for the material model provides a reasonable output for simulating the behaviour of bone during compression, a simple model of 10x10x10 mm cubes is build for the relative densities $\rho_r = 0.2$, $\rho_r = 0.3$, $\rho_r = 0.4$, $\rho_r = 0.5$, and $\rho_r = 0.6$. The volumetric strain at total compaction is found by equation (8.17).

$$\varepsilon_v = ln(\frac{1}{\rho_r}) \tag{8.17}$$

The x and y direction are chosen to be constrained and a forced displacement is applied in the z direction. The initial and final situation of the cubes with different $\rho_r$ is illustrated in figure 8.3, where total compaction is achieved for the various densities.

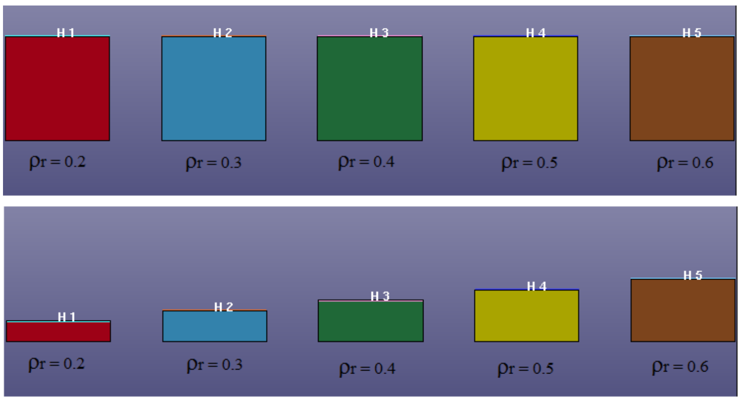


***Figure 8.3.*** Test models to examine the compressive behaviour in bone tissue with different relative densities. The squares to the left is the start situation with different densities before compaction, and the squares to the right is the end situation when fully compacted.

The z-stresses as a function of the time from t=0 to t=0.02 sec. found for the cubes with different relative densities are illustrated in figure 8.4.

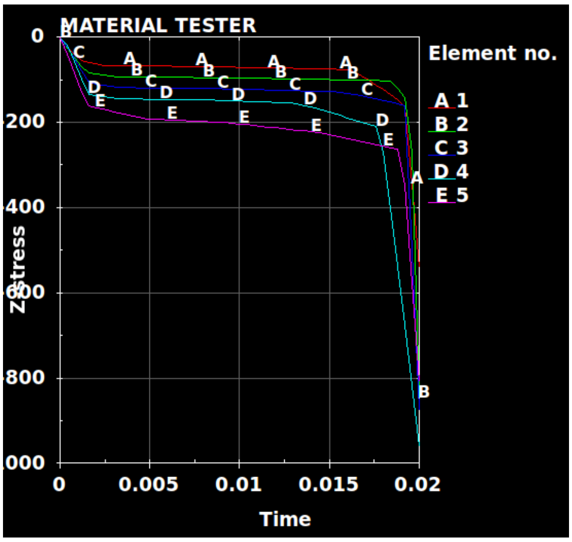


***Figure 8.4.*** Stresses in the z-direction as a function of time for the cubes with different densities, which gives similar behaviour for the trabecular bone as discussed in section 5.2.1

As the x axis is time, the data is converted to express the stress strain as illustrated in figure 8.5, resulting in similar axis as for figure 5.4 and figure 5.3 for a higher comparability of the results and thereby validate the mechanical behaviour.

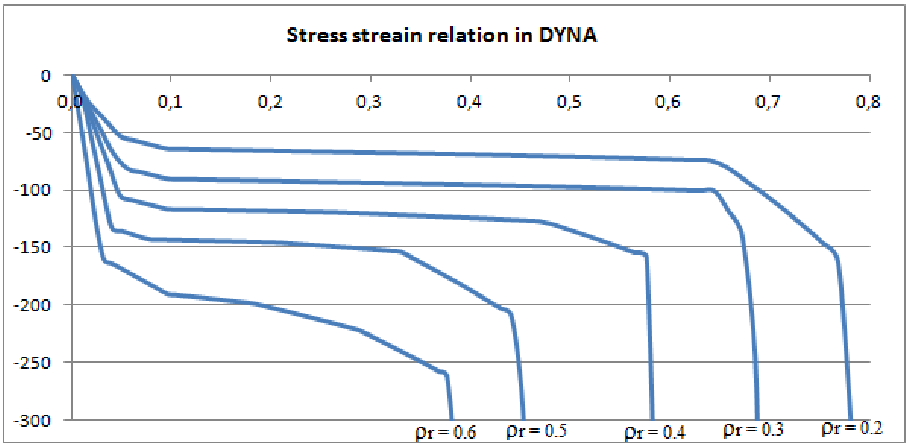


***Figure 8.5.*** The stress strain relation in the test squares in order to validate the compressive behaviour.

Despite of the higher stress values in figure 8.5 compared to figure 5.3 and 5.4, it can be seen that the curves follows similar behaviour, which is essential for using this behaviour in the following modelling process. They all tends with a steep ascent to a flat plateau where the material goes from elastic to plastic deformation. The end behaviour when the bone becomes compact, the curves goes asymptotic against the modulus for bone with a density at 1. The curves are not as smooth, but this is caused by the limited number of assigned points.

As the compressive behaviour in the test squares follows the same trend, but at a too high stress level, they will be used as input for the complex model, as the goal with the model is to describe the behaviour and the physical effect when the bone is exposed to a compressive pressure.It has been chosen to focus on completing the FE model of the compaction process instead of a qualitative geometric regulation.

## 8.3 Preliminary FE model

As the FE is an advanced method for modelling complex problems, it is important that the model is able to provide valid results when changing different parameters. The compressive behaviour found by the analytical model is used for controlling the tendency of the results from the FE model. To ensure that the results continues to be valid, an approach is to build a preliminary model, verify that findings are consistent and then expand the model and ultimately changing the mentioned parameters. This ensures reliable data and thereby a stable model through the modelling process. The analytical model only analysed the compaction process in the trabecular bone. In the FE model the impact of the outer layer of the compact bone is also taken into account. The geometry of the preliminary FE model is illustrated in figure 8.6.

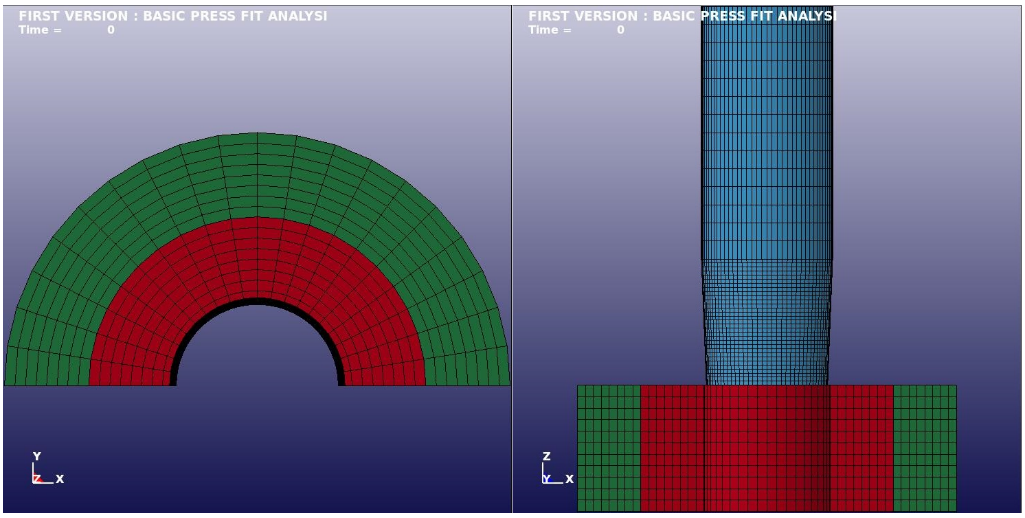


***Figure 8.6.*** The preliminary FE model used for generating a stable process seen from above and from the side. The green illustrates the compact bone, red the trabecular bone and blue the stem.

The model is rotationally symmetrical. The stem is defined to be rigid and have a conical part with a minimum radius smaller than the radius of the hole in the bone, to ensure a smooth process when compacting the bone. A velocity curve is defined and assigned to the stem to simulate the insertion and pull-out. The trabecular bone is assigned with the previous mentioned MAT-005, which is in accordance with the compressive behaviour of bone. The compact bone is chosen to be constrained at the bottom in the z-direction. Snapshots from the simulation of the insertion process and pull out of the stem is illustrated in figure 8.7, from time t=0 to time t=0.0148.

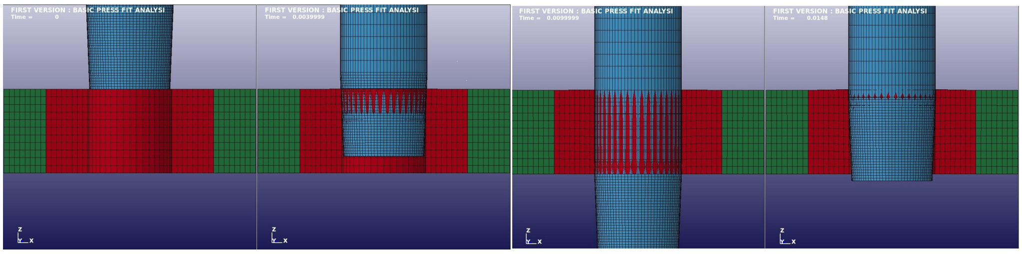

***Figure 8.7.*** Snapshots from the insertion process in the preliminary model over time, of which the first image is the start situation. The second is midway in the insertion process, the third is at total contact between bone and stem, and the fourth image is when contact no longer exist.

The results from the preliminary model during the simulations are of an acceptable behaviour, which is why this model will be used for the additional simulations, but with a few geometric regulations in order to obtain fairly similar geometry as in the analytical model. It can be seen in figure 8.7, that the radius of the trabecular bone and the radius of the stem does not correlate with the dimensions from the analytical model. This choice was made based on that the model was created to evaluate the results in a controlled way.

The geometry is changed for the final FE model, which is illustrated in figure 8.8, of which the geometry of the bone is more consistent with the geometry in the analytical model. The thickness of the compact bone is 3.3 mm, the bottom radius of the stem is 9 mm and the top is 12 mm. But the height of the stem is twice of the analytical in order to ensure a smooth process of bone compaction, which results in a top radius of the stem at 10.5 mm instead of the 12 mm as in the analytical model when inserted. The friction between the stem and bone is set to be 0.1.

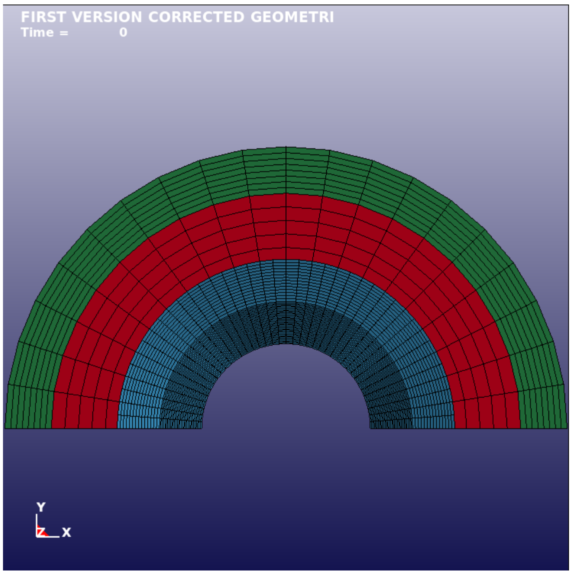


***Figure 8.8.*** The geometry of the final FE model used for simulating the initial stability with changing preconditions. Green is compact bone, red is trabecular bone and blue is the stem.

The model illustrated in figure 8.8 will form the basis for the simulations when changing preconditions.

## 8.4 Simulating different densities

At first the insertion force and the pull-out force is examines bone with the different relative densities analysed in the analytical model, $\rho_r = 0.2$, $\rho_r = 0.3$, $\rho_r = 0.4$, $\rho_r = 0.5$, and $\rho_r = 0.6$. The results from the simulations are illustrated below, of which the first part of the graph with the steep decent indicates the insertion of the stem and the second part with the steep ascent indicates the pull-out of the stem. The highest values in both parts are the insertion force and pull-out force respectively, and illustrated with a $*$.

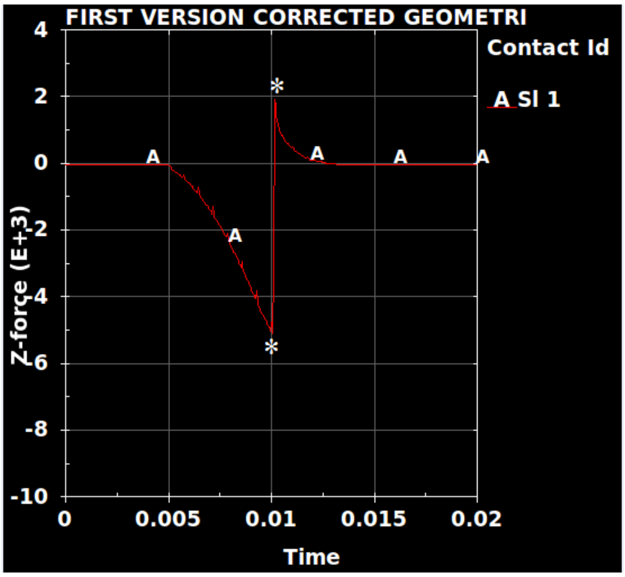


***Figure 8.9.*** The insertion- and pull-out force when inserting the stem in bone with $\rho_r = 0.2$, marked with a $*$.

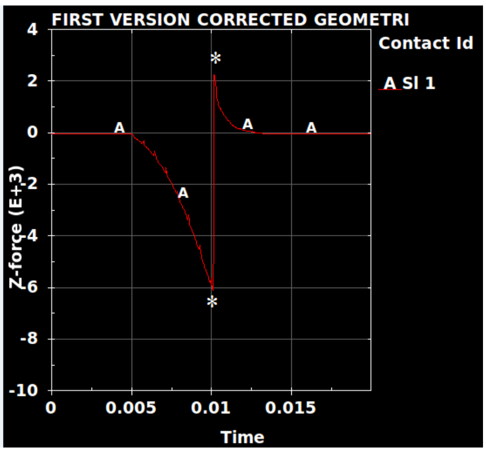


***Figure 8.10.*** The insertion- and pull-out force when inserting the stem in bone with $\rho_r = 0.3$, marked with a $*$.

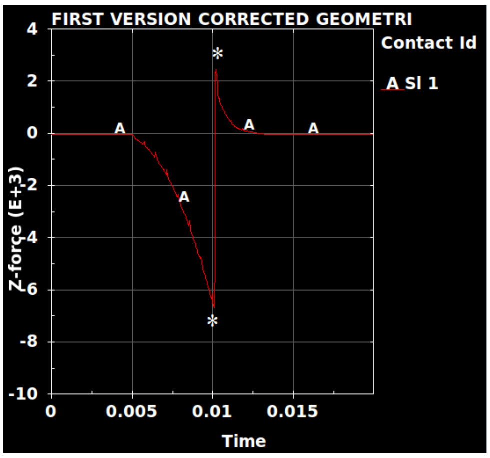


***Figure 8.11.*** The insertion- and pull-out force when inserting the stem in bone with $\rho_r = 0.4$, marked with a $*$.

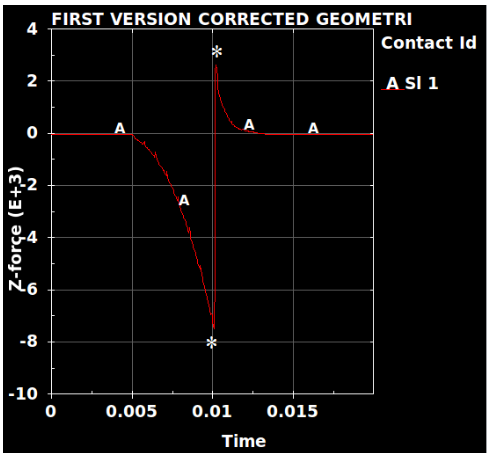


***Figure 8.12.*** The insertion- and pull-out force when inserting the stem in bone with $\rho_r = 0.5$, marked with a $*$.

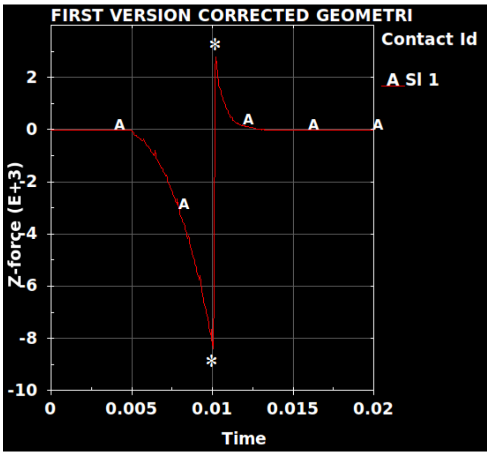


***Figure 8.13.*** The insertion- and pull-out force when inserting the stem in bone with $\rho_r = 0.6$, marked with a $*$.

It can be seen that the insertion force is generally higher than the pull-out force. This can be due to the major force used for the initial process of compacting the bone tissue. The ratio between the insertion force and pull-out force is almost the same in all cases. In $\rho_r = 0.2$ the ratio is 37 %, $\rho_r = 0.3$ is 36 %, $\rho_r = 0.4$ is 35 %, $\rho_r = 0.5$ is 34 %, and $\rho_r = 0.6$ is 36 %. It can thereby be determined that there is an significant correlation between the insertion force and pull-out force. It can also be seen that both the insertion- and pull-out force depends on the magnitude of the relative density, as both increases when $\rho_r$ increases. This indicates that a higher relative density results in a better fixation of the stem.

## 8.5 Simulating geometric changes

In order to investigate the impact of the geometric conditions of the stem with respect to the obtained forces, the geometry was slightly changed by changing the bottom radius to 9.4 mm and the top radius to 11.6 mm, which originally was 9 mm and 12 mm respectively. This results in a smaller conical angle. The simulation was performed with $\rho_r = 0.2$, and the result is illustrated below, of which figure 8.14 is the result with the original stem geometry for comparison, and figure 8.15 is the result with the changed stem geometry.

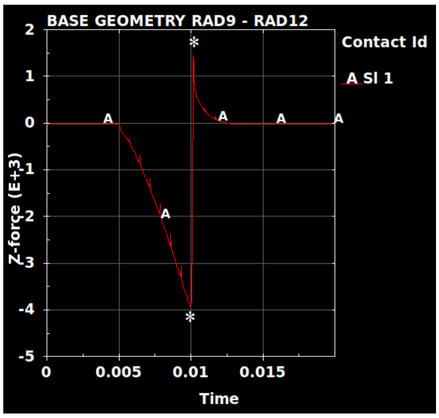


***Figure 8.14.*** The insertion- and pull-out force when inserting the original stem in bone with $\rho_r = 0.2$

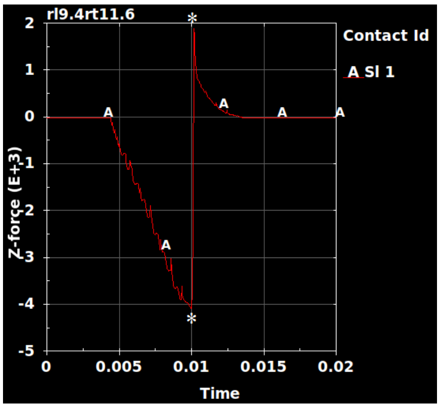


***Figure 8.15.*** The insertion- and pull-out force when changing the stem geometry in bone with $\rho_r = 0.2$

It can be seen that a geometric change have an influence on both the insertion- and the pull-out force. The result when changing $\theta$ to a smaller value results in higher pull-out force, but an almost identical insertion force. It has not been investigated whether the maximum $\sigma_\theta$ changes. The insertion force is slightly increased with 7.6 % and the pull-out force is increased with 26 %. So in principle would an angle of 2.5 °provide a better result when the $\rho_r = 0.2$ instead of the current angle of the stem.

### 8.5.1 Simulating different yield strength

The last parameter investigated in the FE model is the effect of the yield strength modelling. In LS-DYNA the uniaxial yield stress $\sigma_y$ is controlled by three constants, of which the values are chosen based on the desired outcome. These controls the deviator stresses and can include the magnitude of the pressure. $\sigma_y$ is described by equation (8.18).[LSTC, 2007]

$$\sigma_y = [3 * (a_0 + a_1 P + a_2 P^2)]^{1/2} \tag{8.18}$$

The constants $a$, $a_1$ and $a_2$ controls the magnitude of the actual yield strength and thereby how much it affects the yield strength, of which a higher $a$ values results in a higher influence.[LSTC, 2007]

The effect of the yield strength with respect to the insertion force and the pull-out force in $\rho_r = 0.6$ is examined by changing the $a$ constants. At first the constants $a_1 and a_2$ are set to 0, which means that the pressure does not influence the yield strength which results in equation (8.19).[LSTC, 2007]

$$a_0 = \frac{1}{3} * \sigma_y^2. \tag{8.19}$$

Here the yield strength is constant and no pressure effect of the deviatoric response. Then the constants $a_1 and a_2$ are set to be = 2, which means a pretty strong strong influence of the hydrostatic pressure. [LSTC, 2007] The resulting force is illustrated in figure 8.16 and figure 8.17.

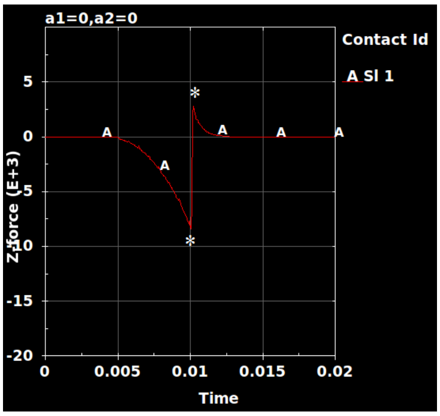


***Figure 8.16.*** The insertion- and pull-out force when changing the yield strength.

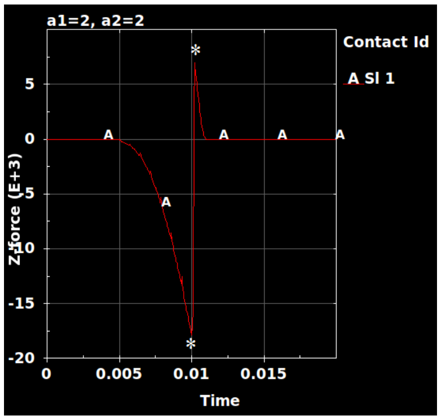


***Figure 8.17.*** The insertion- and pull-out force when changing the yield strength.

It can be seen that pressure dependent yield strength have a major influence on the force response in the model. When the constants were set to be 2, the effect of the pressure is very strong which results in higher forces. The insertion force is approximate 10.000 MPa higher and the pull-out force is 5000 MPa higher. Further studies should be made to find the appropriate values for $a_1 and a_2$.

The results from the FE model indicates similar behaviour as the analytical model, but in a more complex 3D domain and with the outer ring of the compact bone taken into account. Even though further geometric developments would be essential for a more realistic model, the results provides an insight of the consequences when the preconditions of the host bone are changed. As great effort have been made to make sure that the compressive behaviour follows the tendency found in the literature, which is why the results can be used to analyse the qualitative differences of the outcome of a surgical procedure based on the relative density or the geometry of the stem, since the model follows the changing compressive behaviour of bone tissue. Furthermore the model provides the ability of changing the input parameters e.g. yield strength and elastic modulus, which makes further parameters studies easy.

CHAPTER

# 9 Results

In this thesis two mathematical models in the form of an analytical model and a numerical model in the FE domain have been developed in order to investigate the initial stability of the short femoral stem Primoris. This chapter will provide an overview of the results obtained from the models, and a comparison for verifying the results obtained by the FE model.

As the initial stability is depending on the preconditions of the host bone, and the characteristics of the bone tissue often are very different for each individual patient, the effect of different relative densities was examined. In addition different geometric variations of the stem were investigated to find which geometry that provides the best stability. The stability was analysed by estimating the pull-out force of the stem from the bone.

At first the analytical model, which was a simplified model of the problem, was developed to provide an understanding of the compressive behaviour of bone tissue and to obtain quantitative information of the pull-out force when changing the different preconditions, such as the relative density, the amount of trabecular bone, the friction between bone and stem, and the angle of the stem. The analytical model was used as a basis for creating a more complex 3D model of the problem in the FE domain. Here effects of the relative density of the trabecular bone was investigated, along with the effect of geometric changes of the stem, and the effect of changing the yield strength.

In order to create the FE model and verify the results to subsequent expand the model to generate qualitative knowledge of the result of a surgery, the results are compared with the results from the analytical model. Initially the compressive behaviour of the bone tissue was investigated and illustrated in order to validate the behaviour by comparing with the behaviour found in the literature, as this was essential to provide data that reflects the true behaviour of bone when compacted. Despite a higher stress level in the FE model, the compressive behaviour follows similar behaviour as of [Ashby and Gibson, 1999] and [Gibson, 1985] for all relative densities. The initial part of the curves illustrates the elastic behaviour, of which the curves tends to a flat plateau of where the bone tissue collapses and plastic deformation occurs. The end slope is a steep ascent which tends to totally compaction.

As the compressive behaviour is reliable behaviour, it was used for the validation of the subsequent findings. The most varying precondition of the host bone was found to be the relative density, and therefore investigated by both models. The pull-out force was found with a conical angle $\theta$=3.5 °and a friction coefficient at 0.1, in order to compare the behaviour found by both models. The results from the analytical model are illustrated in figure 9.1, and the results from the FE model are illustrated in figure 9.2. As the stress levels in the material behaviour used in the FE model are significantly higher than in the analytical model, it is expected that the estimated pull-out force from the FE model is within a higher range.

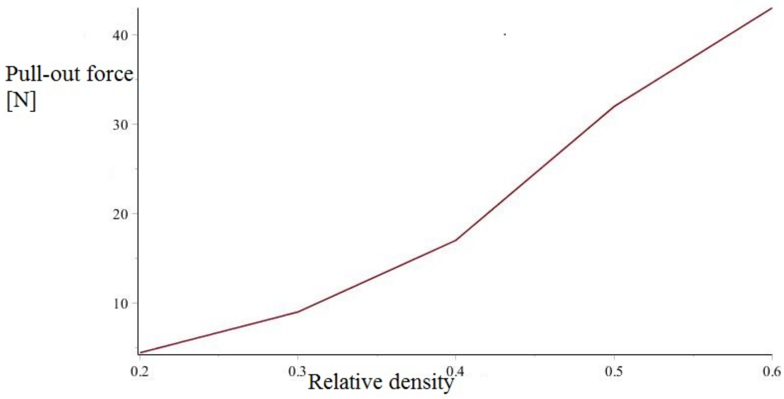


***Figure 9.1.*** The pull-out force as a function of the relative density found analytically.

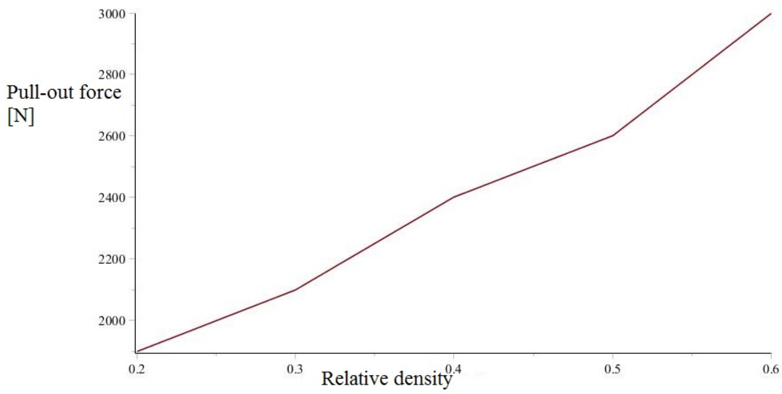


***Figure 9.2.*** The pull-out force as a function of the relative density found by FE modelling.

Despite of the higher stress level in the FE model, which results in a higher pull-out force, a considerable similarity of the behaviour can be seen. The tendency when changing the relative density is almost identical in the two models, but a slightly different slope is present which can be caused by the including of the compact bone in the FE model. The highest pull-out force is obtained by the highest relative density in both models. It can also be seen that the difference in pull-out force increases with the relative density. This makes the results from the FE model reliable, and can therefore be used for further investigations.

When changing the geometry of the stem to a lower conical angle from $\theta$=3.5 °to $\theta$= 2.5 °for bone tissue with a relative density at 0.2 the pull-out force increases with respectively 5 % in the analytical model and 6% in the FE model. This may indicate that the many assumptions made are reasonable, since the models estimates similar behaviour.

The overall similarity of the estimated behaviour of the pull-out force when changing different preconditions of the host bone indicates that the FE model could be a good foundation for further developments and examinations. Material parameters should however be tuned and adjusted to experimental results. To reach a more complete geometry, reasonable informations of the real anatomy should be based on radiographic and density distributions, but with a similar phenomenological treatment.

# Part III

# Synthesis

CHAPTER

# 10 Discussion

This thesis proposes a mathematical method for analysing the process of bone compaction in relation to the initial stability of the femoral prosthesis Primoris. The applied modelling method was Finite Element which was created on the basis of an analytic solution of the compaction problem. In this chapter a discussion of the methodology used for creating the analytic model and the FE model will be presented, and the results obtained from the two models will be discussed. This will be followed by a future perspective.

## 10.1 Methods

Hip arthroplasty is a relative common procedure and has existed for several decades. Along with the advancement of knowledge in the construction and mechanical behaviour of bone tissue and the ability to develop mathematical models for analysis, the procedure has been evolved and investigated a lot. As Primoris is a new small femoral prosthesis, there is only limited research exactly related to it. But a lot of the parameters regarding femoral prosthesis and bone mechanics have been examined by other researchers, which provided the basis for this thesis.

The effect of bone compaction in order to fixate a prosthesis have been investigated by [John R. Green and Balas, 1997] in canines, which states that bone compaction increases the initial stability of the prosthesis compared with conventionally drilling, but based on a cadaver study of 10 femur [Søren Kold and Søballe, 2004] states that this methods often results in fraction of the compact bone, which is why it was chosen to analyse the amount of compaction in relation to the stability of the prosthesis. [Ashby and Gibson, 1999] states that the compressive behaviour of bone is depending on the relative density, which again depends on age, sex, etc., and as no expressions for describing the compressive behaviour exist, it was chosen to generate a mathematical expression based on curve fitting. Here a $3^{rd}$ order polynomial was chosen, as the fit was of the right behaviour. In order to achieve more accuracy in the expression, a higher order could have been chosen, but as the purpose of the analytical model was simplicity is was determines that the $3^{rd}$ order provided an acceptable fit.

As it is very difficult to conduct experiments to measure these parameters, and the analytical model only provides closed-form solutions, a FE model was developed based on the ability of analysing the problem in a more complex domain. FE are also a common method for analysing biomechanical problems e.g. [M. Doblare and Gomez, 2003] has used FE modelling in order to simulate and analyse bone fractures in the hip by using existing literature regarding bone structure and mechanics, and [Guang-Xing chen, 2013] used FE modelling to create a model of the hip which simulates the different bone tissues in order to analyse normal and abnormal loads. But as no studies have been made regarding the compressive behaviour of the trabecular bone when inserting a conical device, the chosen validation method was by comparing with the results from the analytical model.

The initial stability was chosen to be analysed based on the pull-out force. As stated by [Bozkaya and Muftu, 2002], who investigated the metal to metal contact in dental implants, the fit and thereby stability of a conical implant is depending on the contact pressure and corresponding pull out force, which supports the choice of perceiving the problem. [Bozkaya and Muftu, 2002] showed that the geometry of the implant had an influence of the pull-out force, which supports the choice of investigating different stem geometries.

## 10.2 Results

The analytical model showed great variance between the contact pressure and the relative density of the bone tissue which was expected. In the additional calculations, the model showed that higher contact pressure resulted in a higher pull-out force which is supported by [Bozkaya and Muftu, 2002]. It also showed that the geometry and friction between the bone and stem have great influence on the pull-out force.

The results from the FE model of the increasing pull-out force as a function of an increasing relative density was in compliance with the results from the analytical model, but in a higher stress level, which is a result of the chosen material properties. The tendency contained some deviations, especially in the lower densities. As stated by [Andre Freitas and Sahay, -], the results from the FE model is depending on parameters such as the size of the mesh, boundary conditions and material properties. In this case the mesh was chosen relative coarse. A more precise mesh could have been found by conducting a mesh refinement study, however due to the relative simple geometry, this is not vital for the results.

As a considerable effort was made to generate a mathematical expression for the compressive behaviour of the trabecular bone in accordance with the behaviour found in [Ashby and Gibson, 1999], the amount of limitations and thereby the number of assumptions, such as the symmetric geometry, material behaviour, exclusion of the compact bone in the analytical model etc. are considered when analysing the results. As focus was to analyse the overall influence when changing different parameters regarding the precondition of the host bone, in order to evaluate the most effective configuration, these assumptions were neglected. As the model only was an interpretation of the problem, the deviations can be accepted according to [Philip Purcell and Morris, 2014], who states that as focus was to create a basis model to estimate the changing results, the model can be used for further studies by making it more advanced.

## 10.3 Future perspective

As an alternative to in vivo studies, mathematical modelling is a well used option for analysing biomechanical processes, which in this case was the initial stability of a femoral prosthesis. The chosen modelling method was Finite Element, which was created on the basis of an analytical model. But in order to apply the results from the FE model on the actual outcome of a surgical procedure, further studies have to be made, either as in vivo studies or by the usage of sawbone, which is plastic or foam bones with properties similar to real bone for biomechanical or orthopaedic analysis, to confirm the results and test the real biomechanics of the bone tissue in the human hip, and thereby apply these data as input to the FE model.

Focus in this thesis has been the compressive behaviour of the trabecular bone. With the knowledge obtained, a natural next step would be to include evaluation of the compact bone response, in order to be able to predict the risk of fractions by finding the axial limit for the stem radius.

In the models, the femoral metaphysis and the stem were assumed to be rotationally symmetric. To make the model more realistic and thereby the results more applicable for clinical applications, the morphological differences of both bone and stem have to be taken into account. This will provide a possibility of making the model more patient specific and thereby maybe predict the outcome of the procedure preoperative. This will also improve the understanding of the individual biomechanics compared with the current visual method which is templating.

Furthermore the model can be used to test the postoperative effect of the stability, when the patient starts to walk normally again. This could be done by applying cyclical loads to the FE model, which corresponds to the load, that the hip would be exposed to during a normal walk cycle. This could provide important knowledge of the short and long term fixation.

CHAPTER

# 11 Conclusion

The initial stability of a prosthesis during a hip arthroplasty is very important for long-term success. The aim of this thesis was to investigate the compressive behaviour of bone tissue, and thereby the initial stability of the femoral stem Primoris as a function of different preconditions of the host bone. The initial stability was estimated as the pull-out force of the stem from the bone. In order to obtain an understanding of this, a mathematical model was created on the basis of Finite Element modelling to simulate the mechanical behaviour during the bone compaction and the initial stability. To obtain an initial knowledge about the compaction problem and the effect of changing different preconditions, an analytical model was created. This provided an interpretation of the mechanical behaviour, which could be used as a basis for creating the FE model.

Although the models are approximations of the reality, it provides a substantial understanding of how well the stem is fixated, depending on different preconditions. Thereby it can be concluded, that this thesis demonstrates the ability to estimate the initial stability based on different preconditions of the host bone. This knowledge can be useful for further experiments and further developments, which may result in a more complex geometry in accordance to the hip anatomy, since the results are based on the changing compressive behaviour of the trabecular bone. It can also be concluded that the preconditions of the host bone have a significant impact on the pull-out force, with the relative density as the most prominent for a successful result, since the pull-out force is decreasing significantly when the relative density decreases. For low initial densities, significantly higher compaction should be used to reach the same initial stability. Furthermore the geometry of the stem is of influence of the final result, which is why this should be considered to be taken into account in the original stem.

While this approach is not intended to replace an in vivo experiment, as a mathematical model is only an interpretation of the reality, it can be useful for surgeons in order to provide an understanding of the compaction process when dealing with different bone densities and how this will effect the initial stability. Furthermore it can be useful to investigate which stem geometry that provides the best stability. Combined with the knowledge that the surgeon obtains from templating, an interpretation of how to obtain the best fixation without fractions can be made preoperative. The results obtained from the FE model are therefore of significant relevance for future biomechanical research. It may be possible to extract some informations from the analytical model in regard to a moment loading, which could provide informations on a suitable size and angle of the stem for various relative densities.

# Bibliography

**Alexandre Terrier, 2005**. Hiromichi Fujie Kozaburo Hayashi Lalao Rakotomanana Alexandre Terrier, Junpei Miyagaki. *Delay of intracortical bone remodelling following a stress change: A theoretical and experimental study.* page 998–1006, 2005.

**Andre Freitas and Sahay, -**. Joao B. Jares Stefan Decker Andre Freitas, Kartik Asooja and Ratnesh Sahay. *A Semantic Web Platform for Automating the Interpretation of Finite Element Bio-simulations.* pages –, -.

**Ashby and Gibson, 1999**. Michael Ashby and Lorna Gibson. *Cellular solids - structure and properties.* ISBN: 978-0521499118. Pergamon press, 1999.

**Ashman and Turner, 1993**. Jae Rho Richard B. Ashman and Charles H. Turner. *Young's modulus of trabecular and cortical bone material: Ultrasonic and microtensile measurements.* pages 111–119, 1993.

**Boris Zelle and Krettek, 2004**. Torsten Gerich Boris Zelle and Christian Krettek. *Total hip arthoplasty in young patients using the thrust plate prosthesis: clinical and radiological results.* pages 310–316, 2004.

**Bozkaya and Muftu, 2002**. Dincer Bozkaya and Sinan Muftu. *Mechanics of the tapered interference fit in dental implants.* 2002.

**Claus Munk Jensen and Villadsen, 2008**. Nicolai Bang Foss Claus Munk Jensen, Martin Lamm and Birgit Villadsen. *Referenceprogram for Patienter med Hoftebrud*, 2008.

**Dally and Riley, 1987**. James W. Dally and William F. Riley. *Experimental stress analysis.* ISBN: 0-07-015204-7. McGraw Hill Book Co., 1987.

**Den Ortopædiske Fællesdatabase, 2013**. Forskningsleder Søren Overgaard Den Ortopædiske Fællesdatabase. *Dansk Hoftealloplastik Register*, 2013. URL `http://dhr.dk/`.

**Dieppe and Lohmander, 2005**. Paul A Dieppe and Stefan Lohmander. *Pathogenesis and management of pain in osteoarthritis.* page 965–973, 2005.

**Frederic Martini and Bartholomew, 2012**. Judi Nath Frederic Martini and Edwin Bartholomew. *Fundamentals of anatomy and physiology.* ISBN: 0-321-73553-6. Pearson, 2012.

**Gibson, 1985**. L J Gibson. *The mechanical behaviour of cancellous bone.* pages 317–328, 1985.

**Guang-Xing chen, 2013**. Bing-Nin Yu et al. Guang-Xing chen. *A three-dimensional Finiteb Element model for biomechanical analysos of the hip.* pages 803–808, 2013.

**Iain Spears and Hille, 1998**. Martin Pfleiderer Iain Spears, Michael Morlock and Ekkehard Hille. *The influence of friction and interference on the seating of a hemispherical press-fit cup.* pages 1183–1189, 1998.

**John R. Green and Balas, 1997**. Steven Arnoczky John R. Green, Jean Nemzek and Mark Balas. *The effect of bone compaction on early fixation of porous-coated implants.* pages 91–96, 1997.

**Khoei, 2005**. Amir R. Khoei. *Computational Plasticity in Powder Forming Processes - 2. Finite element model.* ISBN: 978-0-08-044636-3. Elsevier, 2005.

**Larry W. Carter and Young, 1995**. Don O. Stovall Larry W. Carter and Timothy R. Young. *Determination of Accuracy of Preoperative Templating of Noncemented Femoral Prostheses.* pages 507–513, 1995.

**LSTC, 2007**. LSTC. *LS DYNA keyword, users manual.* ISBN: 0-9778540-3-5. LSTC, 2007.

**M. Doblare and Gomez, 2003**. J. Garcia M. Doblare and M. Gomez. *Modelling bone tissue fracture and healing: a review.* page 1809–1840, 2003.

**Mont and Hungerford, 1995**. M. Mont and D. Hungerford. *Non-traumatic avascular necrosis of the femoral head.* pages 459 –474, 1995.

**Niklas B. Damm, 2015**. Nicholas E. Bishop Niklas B. Damm, Michael M. Morlock. *Friction coefficient and effective interference at the implant-bone interface.* page 3517–3521, 2015.

**Per Kjærsgaard-Andersen and Søballe, 2006**. Jens Stürup Søren Overgaard Per Kjærsgaard-Andersen, Peter Gebuhr and Kjeld Søballe. *Total Hoftealloplastik - Referenceprogram*, 2006.

**Peter Walker and Casas, 2005**. Daniel de Prada Peter Walker, Gordon Blunn and Cristina Casas. *Design radionale and dimensional considerations for a femoral neck prosthesis.* pages 313–319, 2005.

**Philip Purcell and Morris, 2014**. Fiona McEvoy Stephen Tiernan Philip Purcell, Magdalena Tyndyk and Seamus Morris. *A parametric finite element analysis of the compacted bone–cement interface following balloon kyphoplasty.* page 89–97, 2014.

**Robert Cook and Plesha, 1992**. David Malkus Robert Cook and Michael Plesha. *Concepts and applications of finite element analysis.* ISBN: 0-471-50319-3. Wiley, 1992.

**Scott and Wolfe, 2010**. David L Scott and Frederick Wolfe. *Rheumatoid arthritis.* page 1094–1108, 2010.

**Søren Kold and Søballe, 2004**. Johan Bechtold Søren Kold and Kjeld Søballe. *Importance of pre-clinical testing exemplified by femoral fractures in vitro with new bone preparation technique.* pages 77–82, 2004.

**Søren Kold and Søballe, 2003**. Johan Bechtold Søren Kold and Kjeld Søballe. *Compacted cancelleous bone has a spring-back effect.* pages 591–595, 2003.

# Part IV

# Appendix

APPENDIX

# A X-ray for geometric determinations


***Figure A.1.*** X-ray of left femur with the Primoris stem inserted. The anatomy is used for geometric determinations for the mathematical models.